SANDIA REPORT
SAND88—1144 • UC—261
Unlimited Release
Printed July 1988

Rotor Instrumentation Circuits for the Sandia 34-Meter Vertical Axis Wind Turbine

Herbert J. Sutherland, William A. Stephenson

Prepared by
Sandia National Laboratories
Albuquerque, New Mexico 87185 and Livermore, California 94550
for the United States Department of Energy
under Contract DE-AC04-76DP00789

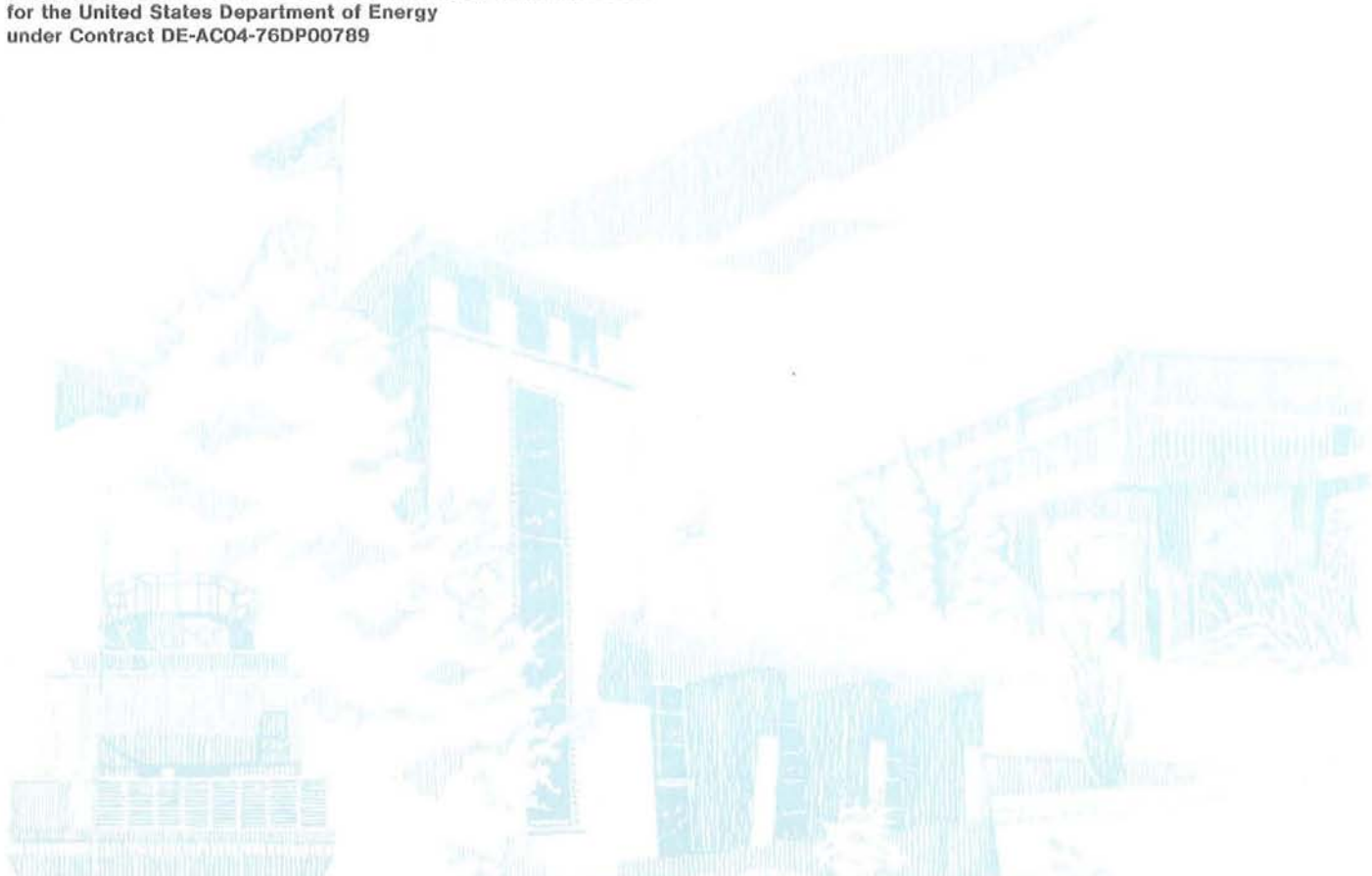

When printing a copy of any digitized SAND Report, you are required to update the markings to current standards.

SF2900Q(8-81)

Issued by Sandia National Laboratories, operated for the United States Department of Energy by Sandia Corporation.

NOTICE: This report was prepared as an account of work sponsored by an agency of the United States Government. Neither the United States Government nor any agency thereof, nor any of their employees, nor any of their contractors, subcontractors, or their employees, makes any warranty, express or implied, or assumes any legal liability or responsibility for the accuracy, completeness, or usefulness of any information, apparatus, product or process disclosed, or represents that its use would not infringe privately owned rights. Reference herein to any specific commercial product, process, or service by trade name, trademark, manufacturer, or otherwise, does not necessarily constitute or imply its endorsement, recommendation, or favoring by the United States Government, any agency thereof or any of their contractors or subcontractors. The views and opinions expressed herein do not necessarily state or reflect those of the United States Government, any agency thereof or any of their contractors.

Printed in the United States of America
Available from
National Technical Information Service
U.S. Department of Commerce
5285 Port Royal Road
Springfield, VA 22161

NTIS price codes
Printed copy: A04
Microfiche copy: A01

Distribution
Category UC-261

SAND88-1144
Unlimited Release
Printed July 1988

ROTOR INSTRUMENTATION CIRCUITS FOR THE SANDIA 34-METER VERTICAL AXIS WIND TURBINE*

by

Herbert J. Sutherland

and

William A. Stephenson

Wind Energy Research Division
Sandia National Laboratories
Albuquerque, New Mexico 87185

ABSTRACT

Sandia National Laboratories has erected a research oriented, 34-meter diameter, Darrieus vertical axis wind turbine near Bushland, Texas, which has been designated the Sandia 34-m VAWT Test Bed. To meet present and future research needs, the machine was equipped with a large array of sensors. This manuscript details the sensors initially placed on the rotor, their respective instrumentation circuits, and the provisions incorporated into the design of the rotor instrumentation circuits for future research. This manuscript was written as a reference manual for the rotor instrumentation of the Test Bed.

* This work was supported by the U. S. Department of Energy at Sandia National Laboratories under contract DE-AC04-76DP00789.

Table of Contents

	Page
ABSTRACT	i
LIST of TABLES	v
LIST of FIGURES	v
LIST of APPENDICES	vi
INTRODUCTION	1
SIGN CONVENTION	2
LAYOUT OF THE INSTRUMENTATION	2
STRAIN GAUGES	2
Strain Gauge Descriptors	2
Circuit Analysis	3
Gauge Factor	3
Wheatstone Bridge Analysis	3
Balanced Bridge	5
Quarter Bridge	5
Axial and Bending Stress State	5
Bending Half Bridge	6
Axial Half Bridge	7
Full Bridge	7
Active and Passive Elements	8
Sign Convention for Stress Measurements	8
Calibration Factors	10
Calibration Resistor	10
Maximum Stress	11
Bending Stress Correction	11
Flatwise Bending	12
Lead-Lag Bending	13
Axial Stress Correction	15
Flatwise Axial	15
Lead-Lag Axial	16
Torque Gauges	16
Gauge Installation	17
Strain Gauge Cables	18
Strain Gauge Cable Descriptors	18
Cable Routes	19
Lead Loss	19
Completion Units	19
Lotus Files	19

Table of Contents (continued)

	Page
DAMAGE GAUGES	20
PRESSURE LINES	20
AUXILIARY CABLES	21
Data Cables	21
Data Cable Descriptors	21
A Cables	22
P Cables	22
Power Cables	22
Video Cables	22
SIGNAL JUNCTION BOX	23
DAAS CABLES	24
FOAMING	24
CONCLUDING REMARKS	24
REFERENCES	27
APPENDICES	28

LIST of TABLES

		Page
Table I.	Active and Passive Elements for the Various Strain Gauge Configurations.	8
Table II.	Section Geometry	12
Table III.	Flatwise Bending Stress Geometry.	13
Table IV.	Lead-Lag Bending Stress Geometry	13
Table V.	Correction Factors for Gauge Circuits	14
Table VI.	Color Codes for the Strain Gauge Circuits	18
Table VII.	Dimensions for the Damage Gauges	21
Table VIII.	Power and Video Cables	23

LIST of FIGURES

Figure 1.	Schematic Diagram of the Instrumentation	1
Figure 2.	Nomenclature for the Rotor Gauges	3
Figure 3.	Notation for the Strain Gauge Circuits	4
Figure 4.	Sign Conventions for the Blade Bending Moments	9
Figure 5.	Schematic Diagram of the Damage Gauges	20
Figure 6.	Nomenclature for the Accelerometer and Pressure Tap Cables	22
Figure 7.	Terminal Block Locations in the Signal Junction Box	23
Figure 8.	Ground Bus and Terminal Layout Plan for Signal Junction Box 1	25

LIST of APPENDICES

		Page
APPENDIX A.	Gauge Circuits for Blade 1	28
APPENDIX B.	Gauge Circuits for Blade 2	29
APPENDIX C.	Gauge Circuits for the Tower.	31
APPENDIX D.	Gauge Circuits for the Brakes.	31
APPENDIX E.	Gauge Circuit Configurations and Gauge Factors for Blade 1	32
APPENDIX F.	Gauge Circuit Configurations and Gauge Factors for Blade 2	33
APPENDIX G.	Gauge Circuit Configurations and Gauge Factors for the Tower.	35
APPENDIX H.	Gauge Circuit Configurations and Gauge Factors for the Brakes	35
APPENDIX I.	Calibration Factors for Blade 1	36
APPENDIX J.	Calibration Factors for Blade 2	37
APPENDIX K.	Calibration Factors for the Tower	39
APPENDIX L.	Calibration Factors for the Brakes	39
APPENDIX M.	Color Codes for Blade 1 Cables	40
APPENDIX N.	Color Codes for Blade 2 Cables	41
APPENDIX O.	Color Codes for the Tower Cables	42
APPENDIX P.	Blade Cable Lengths and Types	43
APPENDIX Q.	Tower Cable Lengths and Types	44
APPENDIX R.	Auxilary Cable Lengths and Types	45
APPENDIX S.	Color Codes and Pin Connections for Cables 12A, 13A, 14A, 15A, 22A, 23A, 24A, 25A, TRA AND TSA	46
APPENDIX T.	Color Codes and Pin Connections for the Cables 14P1, 14P2, 15P1 and 15P2	47
APPENDIX U.	Initial Layout of the Gauges in the Signal Junction Box	48
APPENDIX V.	Initial Layout of the Jumper Cables in the Signal Junction Box	50
APPENDIX W.	Color Codes and Pin Connections for Power Cable SJS1	58
APPENDIX X.	Color Codes and Pin Connections for Signal Cable SJS1	59
APPENDIX Y.	Color Codes and Pin Connections for Signal Cable SJS2	62
APPENDIX Z.	Color Codes and Pin Connections for Signal Cable SJS3	66

INTRODUCTION

Sandia National Laboratories has erected a research oriented, 34-meter diameter, Darrieus vertical axis wind turbine (VAWT) near Bushland, Texas. To meet current and future research needs, the turbine and its environment have been equipped with a large array of sensors, see Fig. 1, to monitor all aspects of the machine's performance. In particular, the instrumentation has been designed to meet three primary objectives: (1) to provide the experimental data required to evaluate the advanced techniques used to design this turbine; (2) to provide experimental data that support current research needs, i.e., modeling of unsteady viscous air flow, fatigue life prediction techniques and system design concepts; and (3) to incorporate sufficient versatility to permit its adaptation to future research needs with minimal difficulty. Current instrumentation includes 70 strain signals from the rotor, 8 strain signals from the brakes, 5 crack propagation signals, 25 environmental signals, 22 turbine performance signals and 29 electrical performance signals. This manuscript discusses the instrumentation that was initially placed on the rotor and the provisions for future research that have been incorporated into its design.

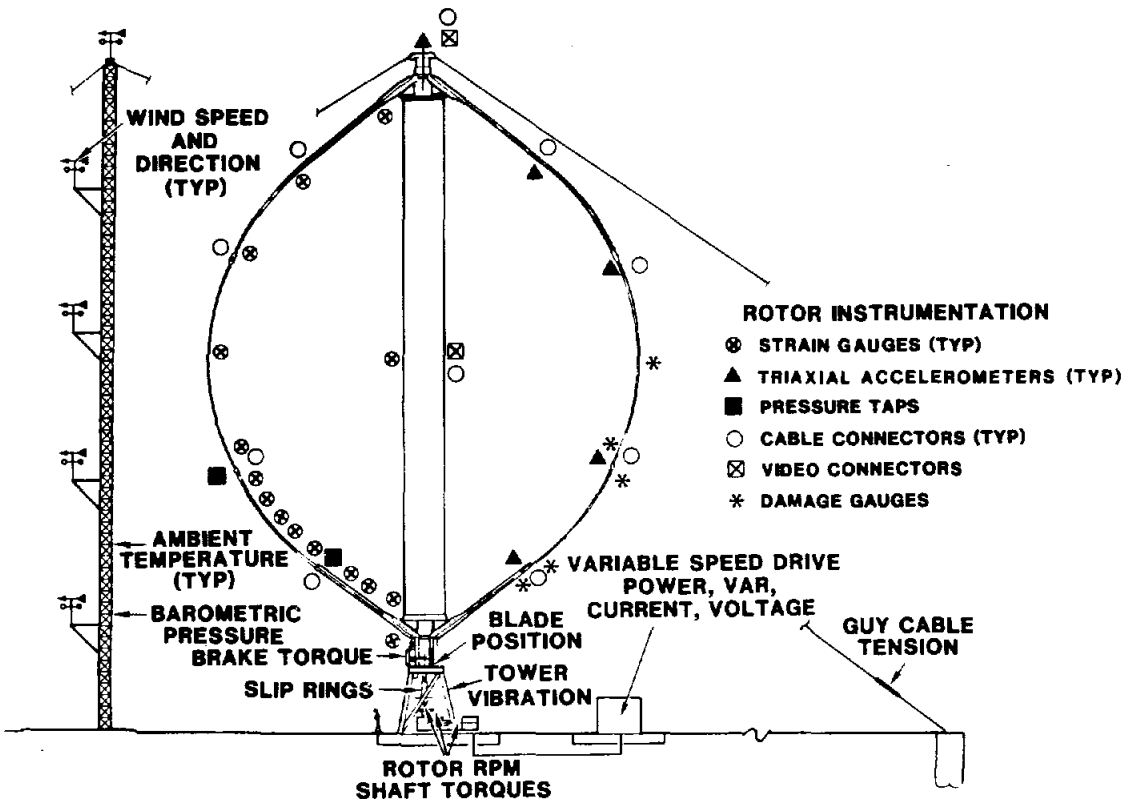

Figure 1. Schematic Diagram of the Instrumentation

SIGN CONVENTION

The sign convention chosen throughout this report is that tension stresses and strains are positive and that compression stresses and strains are negative.

LAYOUT OF THE INSTRUMENTATION

All instrumentation is described in detail in the Sandia drawings numbered S58729, AY-S58729, AY-S68385, S72616, and S72663.

The general philosophy followed in the layout of the instrumentation was to route all of the instrumentation cables to a central location; namely, the bottom, inside of the main tower. At that location, a "signal junction box" is used as a central processing station between the gauge circuits and the data acquisition and analysis system (DAAS).[1]

The many extra cables and pressure tubing, described in detail below, were also brought to the lower, inside of the tower. Because the functions of these extra connections are not defined at this time (they have been installed for future research), they have been terminated inside the tower. Thus, additional connections can be added to the system, as required.

STRAIN GAUGES

The initial set of instrumentation placed on the Test Bed rotor is primarily composed of strain gauges. The strain gauge circuits are summarized in Appendices A through H.

The strain gauges have been placed strategically about the rotor. Major groups of gauges are located about the blade joints and at the equator of the turbine. Strain gauge categories on the blade include flatwise (spanwise) bending, lead-lag (chordwise) bending, and axial (along the span) stress circuits on the blade, see Fig. 4. On the tower and the low speed shaft, categories include rosette, torque, axial, in-plane bending (plane of the blades), and out-of-plane bending circuits (perpendicular to the plane of the blades). All strain gauges were obtained from Micro-Measurements.[2]

Strain Gauge Descriptors

All strain gauges have been designated by their position and their circuit. The key to the nomenclature used in this system is as follows:

First Letter or Number (see Fig. 2):
- 1 : Blade 1
- 2 : Blade 2
- T : Tower/Shaft
- B : Brake

Second Letter or Number (see Fig. 2):
- A through U, and X: Gauge Section
- N, S, E or W: Brake Location

Final Letters or Numbers:
- xxML : Moment Pair in the "Lead-Lag" Position
- xxMF : Moment Pair in the "Flatwise" Position
- xxAL : Axial Pair in the "Lead-Lag" Position

xxAF : Axial Pair in the "Flatwise" Position
xxDL : Direct Strain in the "Lead-Lag" Position
xxDF : Direct Strain in the "Flatwise" Position
xxRA : Rosette Gauge Along the Longitudinal Axis
xxRB : Rosette Gauge 45° to the Longitudinal Axis
xxRC : Rosette Gauge Perpendicular to the Long. Axis
xxF1 : Direct Strain (for the Damage Gauge)
xxAL : Axial Pair on the Lower Brake Caliper
xxAU : Axial Pair on the Upper Brake Caliper

The circuit descriptors are keyed to Fig. 2 and are shown in the detailed Sandia drawings listed earlier. As seen in the these tables, 78 gauge circuits are available for interrogation: 25 on Blade 1, 32 on Blade 2, 13 on the tower, and 8 on the brakes.

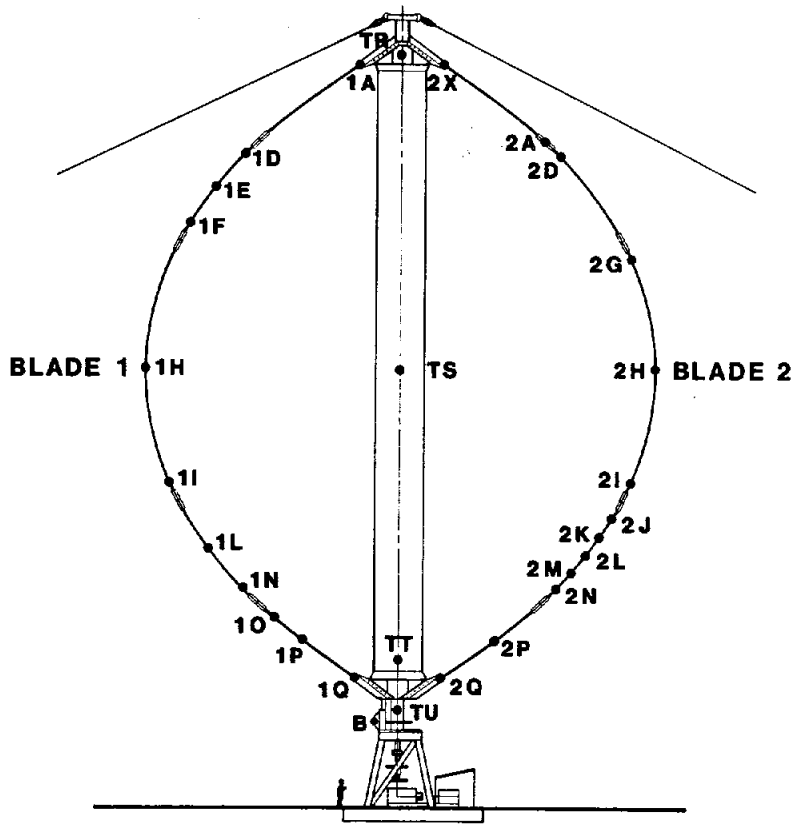

Figure 2. Nomenclature for the Rotor Gauges

Circuit Analysis

The conventional Wheatstone Bridge, see Fig. 3, is used in this installation for all of the strain gauge circuits. The analysis of the circuit may be found in many references (e.g., see Refs. 3, 4 and 5). The analysis is duplicated here for completeness.

<u>Gauge Factor</u>: For the strain gauges used here, the change in gauge resistance δR is related to the strain ε in the gauge by the gauge factor k through the following relationship:

$$k = \frac{\delta R/R}{\delta l/l} = \frac{1}{\varepsilon}\frac{\delta R}{R} \quad . \quad (1)$$

where R is the gauge resistance, δl is the change in the gauge length, and l is the original gauge length.

<u>Wheatstone Bridge Analysis</u>: All bridge circuits were wired according to the "Western Regional" convention that is shown in Fig. 3. For this circuit, the excitation voltage is E (with the polarity indicated), V is the signal voltage (with the polarity indicated), and the resistance of each leg is R_A, R_B, R_C, and R_D, respectively.

This circuit may be analyzed using simple circuit analysis. If the current in each leg is i_A, i_B, i_C, and i_D, respectively, and the voltage drop through each leg is V_A, V_B, V_C, and V_D, respectively, then

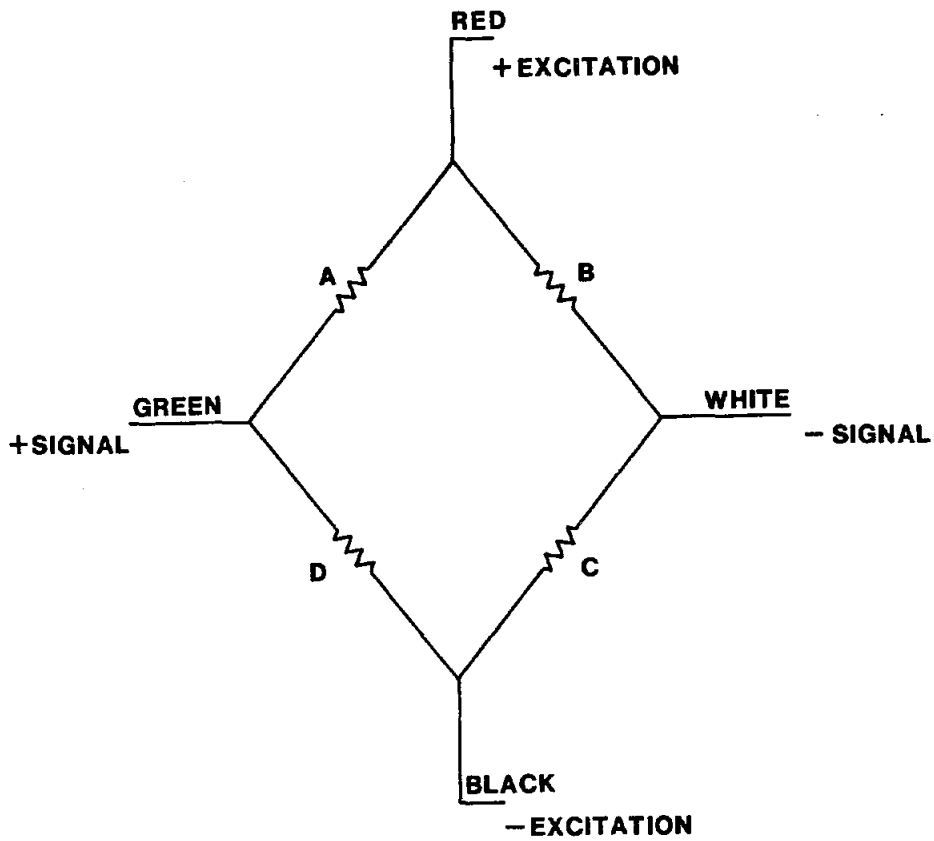

Figure 3. Notation for the Strain Gauge Circuits

$$V_A = i_A R_A \quad , \qquad V_B = i_B R_B$$
$$V_C = i_C R_C \quad , \qquad V_D = i_D R_D \qquad . \quad (2)$$

The signal voltage V is given by

$$V = V_B - V_A = V_D - V_C \qquad . \quad (3)$$

Measuring V with a high impedance device implies that the current in the signal circuit can be neglected and that

$$i_A = i_D = E \,/\, (R_A + R_D) \qquad , \quad (4)$$

$$i_B = i_C = E \,/\, (R_B + R_C) \qquad , \quad (5)$$

$$i = i_A + i_B = i_C + i_D \qquad . \quad (6)$$

Solving Eqs. 2 through 6 for V yields

$$V = E \frac{R_B (R_A + R_D) - R_A (R_B + R_C)}{(R_A + R_D) (R_B + R_C)} \quad . (7)$$

Balanced Bridge: The bridge is said to be balanced when V is zero. Solving Eqs. 2 through 7 for this case yields

$$\frac{R_A}{R_D} = \frac{R_B}{R_C} \quad . (8)$$

Quarter Bridge: For "matched" strain gauges in each arm of the bridge, the nominal resistance of each is R. In the quarter bridge circuit one gauge is subjected to the strain field and the other three are left unstrained; i.e., there is one active element and three passive ("dummy") elements. Thus, when the circuit is strained, the resistance of one element is changed by δR; i.e.,

$$R_A = R_B = R_C = R$$
$$R_D = R + \delta R \quad . (9)$$

Using these values in Eq. 7 and assuming that $|\delta R| << R$ yields:

$$V = E \frac{1}{4} \frac{\delta R}{R} = E \frac{n}{4} \frac{\delta R}{R} \quad . (10)$$

Here, we have chosen to write the number of active elements in this circuit explicitly as n. For this case, n = 1. Substituting this result into Eq. 1 yields:

$$\varepsilon = 4 \frac{1}{E} \frac{1}{k} V = \frac{4}{n} \frac{1}{E} \frac{1}{k} V \quad . (11)$$

Axial and Bending Stress State: For this discussion let us assume that the strain state at the gauge section is composed of two components: bending and tension. Then, the total strain state at station n, ε_n, can be written as:

$$\varepsilon_n = \varepsilon_a + \varepsilon_b \quad , (12)$$

where ε_a is the axial component of strain and ε_b is the bending component of strain. For two stations, with station 1 on the positive side of the neutral axis, station 2 on the negative side and with both stations equidistant from the neutral axis, then[4]

$$\varepsilon_1 = \varepsilon_a + \varepsilon_b = \varepsilon_a - \varepsilon_b$$
$$\varepsilon_2 = \varepsilon_a - \varepsilon_b = \varepsilon_a + \varepsilon_b \quad , \quad (13)$$

or

$$\varepsilon_1 + \varepsilon_2 = 2\ \varepsilon_a \quad , \quad (14)$$

$$\varepsilon_2 - \varepsilon_1 = 2\ \varepsilon_b \quad . \quad (15)$$

Thus, by adding the strain signal from opposite sides of the neutral axis, only axial strains are obtained, Eq. 14; and by subtracting them, only bending strains are obtained, Eq. 15. As the strain is directly related to the change in resistance, Eq. 1, then Eqs. 13 and 14 imply that

$$\delta R_1 = \delta R_a + \delta R_b = \delta R_a - \delta R_b$$
$$\delta R_2 = \delta R_a - \delta R_b = \delta R_a + \delta R_b \quad , \quad (16)$$

or

$$\delta R_1 + \delta R_2 = 2\ \delta R_a \quad , \quad (17)$$

$$\delta R_2 - \delta R_1 = 2\ \delta R_b \quad , \quad (18)$$

where the subscripts in Eqs. 13 through 15 have the same meaning as those in Eqs. 16 through 18.

<u>**Bending Half Bridge**</u>: For "matched" strain gauges in each arm of the bridge, the nominal resistance of each is R. In the half bridge circuit two gauges are subjected to the strain field and the other two are left unstrained; i.e., two active element and two passive ("dummy") elements. If the two active elements are A and D, then when the circuit is strained, the resistance of each active element is changed by δR_A and δR_D, respectively; i.e.,

$$R_B = R_C = R$$
$$R_A = R + \delta R_A \quad , \quad R_D = R + \delta R_D \quad . \quad (19)$$

For bending circuits, gauges D and A are placed on opposite sides of the neutral axis and are equidistant from it, see Eq. 13. Using these values in Eq. 7 and assuming that $|\delta R_A| << R$ and $|\delta R_D| << R$ yields:

$$V = E\ \frac{\delta R_D - \delta R_A}{4\ R} = E\ \frac{2}{4}\ \frac{\delta R_b}{R} = E\ \frac{n}{4}\ \frac{\delta R_b}{R} \quad . \quad (20)$$

Thus, the bending gauge circuit "subtracts" the strain signals from the two active gauges and $\delta R_D - \delta R_A = 2\ \delta R_b$. Again, we have chosen to write the number of active elements in

this circuit explicitly as n. For this case, n = 2. Substituting these results into Eq. 1 and solving for the bending strain ε_b yields:

$$\varepsilon_b = 2 \frac{1}{E}\frac{1}{k} V = \frac{4}{n}\frac{1}{E}\frac{1}{k} V \qquad . \quad (21)$$

Axial Half Bridge: For "matched" strain gauges in each arm of the bridge, the nominal resistance of each is R. In the half bridge circuit two gauges are subjected to the strain field and the other two are left unstrained; i.e., two active element and two passive ("dummy") elements. If the two active elements are B and D, then when the circuit is strained, the resistance of each active element is changed by δR_B and δR_D, respectively; i.e.,

$$R_A = R_C = R$$
$$R_B = R + \delta R_B \quad , \quad R_D = R + \delta R_D \qquad . \quad (22)$$

For axial strains, gauges B and D are placed on opposite sides of the neutral axis and are equidistant from it, see Eq. 13. Using these values in Eq. 7 and assuming that $|\delta R_B| << R$ and $|\delta R_D| << R$ yields:

$$V = E \frac{\delta R_D + \delta R_B}{4\ R} = E \frac{2}{4}\frac{\delta R_a}{R} = E \frac{n}{4}\frac{\delta R_a}{R} \qquad . \quad (23)$$

Thus, the axial gauge circuit "adds" the strain signals from the two active gauges and $\delta R_B + \delta R_D = 2\ \delta R_a$. Again, we have chosen to write the number of active elements in this circuit explicitly as n. For this case, n = 2. Substituting these results into Eq. 1 and solving for the axial strain ε_a yields:

$$\varepsilon_a = 2 \frac{1}{E}\frac{1}{k} V = \frac{4}{n}\frac{1}{E}\frac{1}{k} V \qquad . \quad (24)$$

Full Bridge: For "matched" strain gauges in each arm of the bridge, the nominal resistance of each is R. In the full circuit four gauges are subjected to the strain field and no gauges are left unstrained; i.e., four active elements. For this configuration, the gauges are placed in the strain field so that two are placed in tension and two are placed in compression. When the circuit is strained, the resistance of each active element is changed by δR; i.e.,

$$R_A = R - \delta R \quad , \quad R_C = R - \delta R$$
$$R_B = R + \delta R \quad , \quad R_D = R + \delta R \qquad . \quad (25)$$

Using these values in Eq. 7 and and assuming that $|\delta R| << R$ yields:

Again, we have chosen to write the number of active elements in this circuit explicitly as n. For this case, n = 4. Substituting these results into Eq. 1 and solving for the strain ε yields:

$$\varepsilon = 4 \frac{1}{E}\frac{1}{k} V = \frac{4}{n}\frac{1}{E}\frac{1}{k} V \quad . \quad (27)$$

<u>Active and Passive Elements</u>: Thus, by judiciously choosing active (strained) and passive (unstrained) elements in the Wheatstone Bridge, the circuit can be used to measure specific types of strains. The active and passive elements (gauges), keyed to Fig. 3, are summarized in Table I.

The passive gauges used to complete the bridge circuit were pre-mounted gauges supplied as "completion units" BCNA-2-HB-350 or BCNA-3U-QB-350.[2] The units were placed near the active gauges.

Table I. Active and Passive Elements for the Various Strain Gauge Configurations.

Stain Gauge Configuration	Active Elements	Passive Elements
Bending Pair	A D	B C
Axial Pair	B D	A C
Single	D	A B C
Torque	A B C D	

Sign Convention for Stress Measurements

The same sign configuration was used throughout the strain gauge circuits. For single gauge configurations, the active gauge was placed in the D position. Thus, tension in the gauge produces a positive output voltage; i.e., Eqs. 1, 9 and 10 imply that

$$\varepsilon > 0 \quad \Rightarrow \quad \delta R > 0 \quad \Rightarrow \quad V > 0 \quad , \quad (28)$$

and that compression produces a negative output.

For the bending gauges, the active gauge A was placed in position 1 and the active gauge D was placed in position 2, see Eqs. 13 through 16. As the signals from these two gauges are subtracted from each other, Eq. 20, a tensile component of the bending strain in gauge D and compressive component in gauge A produces a positive output; i.e.,

$$\left.\begin{array}{l} (\varepsilon_b)_D > 0 \;\Rightarrow\; (\delta R_b)_D > 0 \\ (\varepsilon_b)_A < 0 \;\Rightarrow\; (\delta R_b)_A < 0 \end{array}\right\} \Rightarrow (\delta R_D - \delta R_A) > 0 \;\Rightarrow\; V > 0 \quad . \quad (29)$$

And, a compressive component in gauge D and tensile component in gauge A produces a negative output. Note that the axial component of the strain "subtracts" to zero in this configuration, Eq. 16.

For flatwise bending circuits on the blades, gauge D was placed on the outside fibers of the blade (i.e., $y_2 > 0$, see Fig. 4) and gauge A was placed on the inside fiber (i.e., $y_1 < 0$, see Fig. 4), thus positive outputs are obtained when the outside fibers of the blade are in tension, see Fig. 4. For lead-lag bending circuits on the blades, gauge D was placed on the leading edge fibers of the blade (i.e., $x_2 > 0$, see Fig. 4) and gauge A was placed on the lagging edge fibers (i.e., $x_1 < 0$, see Fig. 4), thus positive outputs are obtained when the leading edge fibers of the blade are in tension, see Fig. 4.

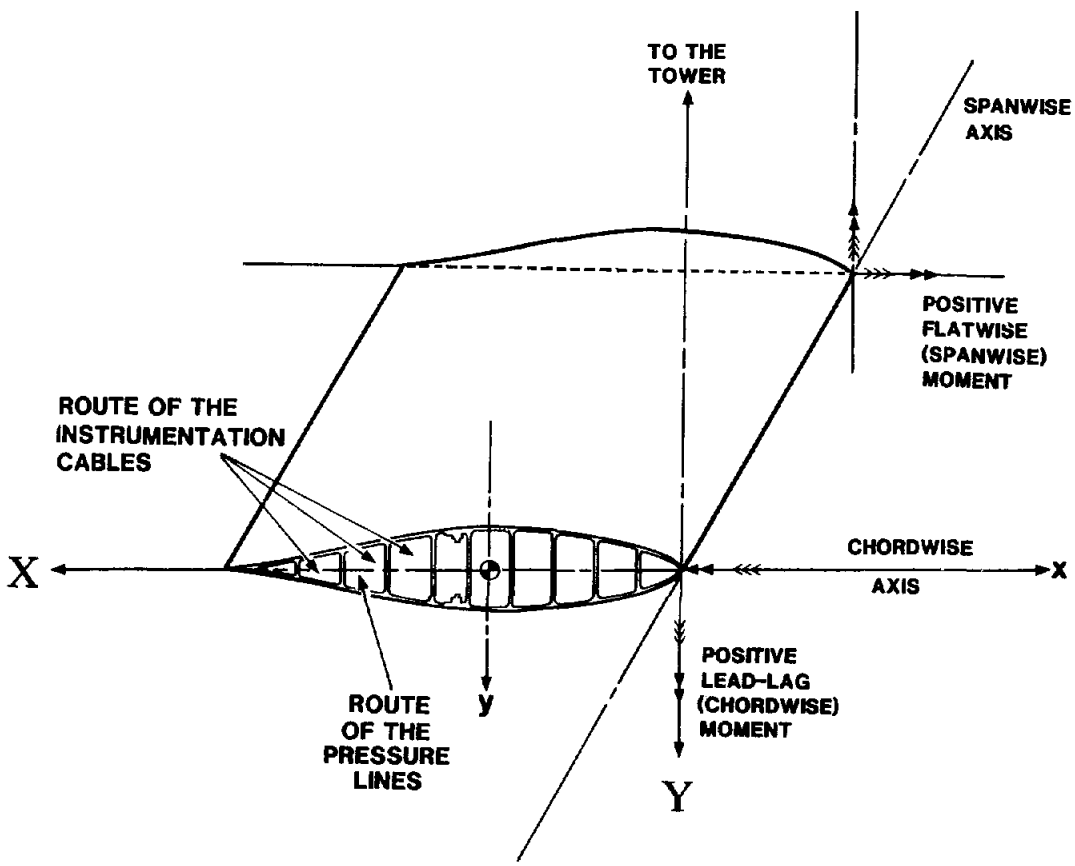

Figure 4. Sign Conventions for the Blade Bending Moments

For the axial gauges, the active gauge B was placed in position 1 and the active gauge D was place in position 2, see Eqs. 13 through 16. As the signals from these two gauges are added, see Eq. 23, a tensile component of axial strain in gauge B and in gauge D produces a positive output; i.e., for stations B and D,

$$\left.\begin{array}{l}(\varepsilon_a)_B > 0 \;\Rightarrow\; (\delta R_a)_B > 0 \\ (\varepsilon_a)_D > 0 \;\Rightarrow\; (\delta R_a)_D > 0\end{array}\right. \Rightarrow \quad (\delta R_B + \delta R_D) > 0 \;\Rightarrow\; V > 0 \quad , \quad (30)$$

and a compressive component in both gauges produces a negative output. Note that the bending component of the strain "adds" to zero in this configuration.

Calibration Factors

For the DAAS system[1] to convert the digital output of its interrogation circuits into the strain (stress) level measured by a strain gauge circuit, a calibration factor is required. For our case, the calibration factor f is defined by

$$\sigma = f\ C \qquad , (31)$$

where C is the number of counts measured by the interrogation circuit. If Y is the modulus of the material on which the strain gauge circuit is attached, A is the amplification of the voltage signal by the DAAS system, and C_V is the number of counts per volt of input, then

$$f = \sigma / C \qquad , (32)$$

$$= Y\ \varepsilon / C \qquad , (33)$$

$$= Y \frac{\delta R / R}{k} \frac{1}{A\ V\ C_v} \qquad , (34)$$

$$= \frac{Y}{A} \frac{1}{k} \frac{\delta R / R}{V\ C_v} \qquad , (35)$$

$$= Y \frac{1}{A} \frac{1}{k} \frac{1}{E} \frac{4}{n} \frac{1}{C_v} \qquad , (36)$$

where n is the number of active elements (gauges) in the strain circuit, see Eqs. 10, 20, 23 and 26. For the system and materials used here, typical values for these constants are A = 250, C_V = 2000, E = 10 volts, and Y = 10E6 psi for aluminum and 30E6 psi for steel. Values for the gauge constant k are listed in Appendices E through H. To convert Eq. 36 from psi units to Mpa units requires the introduction of a units' conversion factor C_u = 6.894757E-3 Mpa/psi. Thus,

$$f = Y \frac{1}{A} \frac{1}{k} \frac{1}{E} \frac{4}{n} \frac{1}{C_v}\ C_u \qquad . (37)$$

<u>Calibration Resistor</u>: To check the output of the gauge circuit, a common practice is to shunt one leg of the bridge circuit with a resistor of a known value. If the shunt resistor has a resistance of R_S and the gauge has a resistance of R, then the circuit is unbalanced by a resistance δR_S that is given by

$$\delta R_s = \frac{R^2}{R + R_s} \quad . \quad (38)$$

Substituting this equation into the above equations yields an amplified calibration voltage of V_c

$$V_c = E \frac{1}{4} \frac{\delta R_s}{R} A \quad . \quad (39)$$

and a calibration stress σ_c of

$$\sigma_c = Y \frac{1}{k} \frac{4}{n} \frac{\delta R_s}{R} C_u \quad . \quad (40)$$

One should note that since the shunt resistor is only placed on one leg of the bridge, the output voltage will be the same for all strain gauge circuits. A typical value for the shunt resistor is 120 kΩ.

<u>Maximum Stress</u>: Most A/D converters can read voltages only over a certain range. If this range is $\pm V_m$, then the maximum stress that can be read by the circuit is limited to

$$\sigma_m = Y \frac{1}{A} \frac{1}{k} \frac{1}{E} \frac{4}{n} C_u V_m \quad . \quad (41)$$

A typical value for the voltage range is ± 5 v.

Bending Stress Correction

As described in the derivation of Eqs. 14 and 15, the above analysis for bending stress is based on bending in a single direction and on symmetric placement of the gauges about the neutral axis of bending. However, neither criterion is true for the lead-lag gauges. The bending in the blades has two components, M_f in the flatwise direction and M_l in the lead-lag. Thus, the total bending moment M_T at a cross section is given by the vector sum

$$\bar{M}_T = \bar{M}_f + \bar{M}_l \quad . \quad (42)$$

Thus, the total bending stress $(\sigma)_m$ measured by a bending strain gauge circuit is given by

$$(\sigma)_m = \frac{M_f}{I_f} \frac{(y_2 - y_1)}{2} + \frac{M_l}{I_l} \frac{(x_2 - x_1)}{2} \quad , \quad (43)$$

where I_f and I_l are the respective moments of inertia, y_1 and y_2 are the perpendicular distances from the flatwise neutral axis to stations 1 and 2, respectively, and x_1 and x_2 are the perpendicular distances from the lead-lag neutral axis to stations 1 and 2, respectively, see Fig. 4. In terms of the maximum stress from flatwise bending σ_{fb} and the maximum stress from lead-lag bending σ_{lb}, Eq. 43 may be rewritten as

$$(\sigma)_m = \sigma_{fb} \frac{(y_2 - y_1)}{2\ y_m} + \sigma_{lb} \frac{(x_2 - x_1)}{2\ x_m} \quad , \quad (44)$$

where $(\sigma)_m$ is the bending stress measured by the gauge circuit, y_m is the perpendicular distance from the flatwise neutral axis to the point where σ_{fb} occurs, and x_m is the perpendicular distance from the lead-lag neutral axis to the point where σ_{lb} occurs. The dimensions for the gauge placement are summarized in Tables II, III, and IV. Two coordinate systems are used in this discussion. The **XY** system has its origin at the leading edge centerline of the airfoil and the xy system has its origin at the neutral axes of the airfoil, see Fig. 4. The transformation between the two system sets of coordinates is given by:

$$\begin{aligned} x_1 &= X_o - X_1 \quad , \quad & y_1 &= Y_1 - Y_o = Y_1 \\ x_2 &= X_o - X_2 \quad , \quad & y_2 &= Y_2 - Y_o = Y_2 \end{aligned} \quad , \quad (45)$$

Flatwise Bending: For the flatwise bending circuit, the gauges were placed symmetrically about the flatwise bending axis and at the same station with respect to the lead-lag bending axis; i.e., $y_2 = - y_1 = y_m$ and $x_2 = x_1$, see Tables II and III. Substituting these values into Eq. 44 yields:

$$(\sigma_{fb})_m = \sigma_{fb} \frac{(y_m + y_m)}{2\ y_m} + \sigma_{lb} \frac{(x_2 - x_2)}{2\ x_m} = \sigma_{fb} \quad . \quad (46)$$

Thus, the measured flatwise bending stress equals the maximum flatwise bending stress at that station.

Table II. Section Geometry

Chord Length m (in)	X_o mm (in)	Y_o mm (in)	x_m mm (in)	y_m mm (in)
0.914 (36)	431.3 (16.98)	0.00 (0.00)	483.1 (19.02)	82.3 (3.24)
1.067 (42)	501.7 (19.75)	0.00 (0.00)	565.2 (22.25)	96.0 (3.78)
1.219 (48)	553.0 (21.77)	0.00 (0.00)	666.2 (26.23)	128.0 (5.04)

Table III. Flatwise Bending Stress Geometry.

Chord Length m (in)	$-Y_1$ Y_2 mm (in)	X_1 X_2 mm (in)
0.914 (36)	82.30 (3.240)	392.13 (15.438)
1.067 (42)	96.11 (3.784)	448.46 (17.656)
1.219 (48)	127.99 (5.039)	373.08 (14.688)

Table IV. Lead-Lag Bending Stress Geometry.

Chord Length m (in)	X_1 mm (in)	$-Y_1$ mm (in)	X_2 mm (in)	$-Y_2$ mm (in)
0.914 (36)	903.27 (35.562)	6.375 (0.251)	6.934 (0.273)	9.525 (0.375)
1.067 (42)	1054.1 (41.500)	4.775 (0.188)	6.934 (0.273)	9.525 (0.375)
1.219 (48)	1206.5 (47.500)	6.350 (0.250)	3.124 (0.123)	18.72 (0.737)

<u>**Lead-Lag Bending**</u>: For the lead-lag bending circuit, aerodynamic and structural considerations prevented the active gauges from being placed at the same position relative to either neutral axis, see Tables II and IV. Thus, the lead-lag bending stress must be corrected for non-symmetry and for "cross talk" with flatwise bending stress. Noting that $|y_2| > |y_1|$ and that both y_1 and y_2 are negative for the lead-lag bending gauges, see Table IV, Eq. 44 may be solved for the measured lead-lag bending stress σ_m in the following form:

$$(\sigma_{lb})_m = - \sigma_{fb} \frac{|\delta y|}{y_m} + \sigma_{lb} \frac{x_{av}}{x_m} \quad , \quad (47)$$

where the variables $|\delta y|$ and x_{av} are defined to be

$$|\delta y| = \frac{|y_2 - y_1|}{2} = \frac{|y_2| - |y_1|}{2} \quad , \quad (48)$$

$$x_{av} = \frac{x_2 - x_1}{2} = \frac{|x_2| + |x_1|}{2} \quad . \quad (49)$$

$(\sigma_{lb})_m$ is the measured lead-lag bending stress and σ_{fb} is the flatwise bending stress at the same gauge section. The variables δy and x_{av} may be calculated using Eq. 45 and the values listed in Table II and IV. We have chosen to write both correction terms in this form for two reasons. First, this permits us to write geometric correction terms that are always positive, see below. And, second, this form permits us to emphasize their sign; namely, a positive flatwise bending moment will decrease the measured lead-lag bending strain.

If we let the geometric correction factor in the two directions be defined as

$$C_{lbf} = \frac{|\delta y|}{y_m} \qquad C_{lbl} = \frac{x_{av}}{x_m} \quad , \quad (50)$$

then, solving for the lead-lag stress yields

$$\sigma_{lb} = \frac{1}{C_{lbl}} (\sigma_{lb})_m + \frac{C_{lbf}}{C_{lbl}} \sigma_{fb} \quad . \quad (51)$$

The values of C_{lbl} and C_{lbf} are listed in Table V. The other terms in Table V will be described later.

The first term of Eq. 51 may be incorporated into the calibration factor directly. Performing the same analysis as cited in Eqs. 32 through 37 yields

Table V. Correction Factors for Gauge Circuits

Chord Length in	C_{lbl} Eq. 50 Eq. 51	C_{lbf} Eq. 50 Eq. 51	C_{fal} Eq. 58	C_{laf} Eq. 60	C_{lal} Eq. 60
36	0.92768	0.01914	0.18833	0.09660	0.05797
42	0.92645	0.02474	0.20647	0.07447	0.06128
48	0.90311	0.04831	0.43970	0.09792	0.09220

$$f = Y \frac{1}{A} \frac{1}{k} \frac{1}{E} \frac{4}{n} \frac{1}{C_v} \frac{C_u}{C_g} \quad , \quad (52)$$

where C_g is the geometric correction factor that is defined to

$$C_g = C_{lbl} \quad \text{for Lead-Lag Bending Circuits}$$

$$C_g = 1 \quad \text{for all other Circuits} \quad . \quad (53)$$

And, Eqs. 40 and 41 become

$$\sigma_c = Y \frac{1}{k} \frac{4}{n} \frac{\delta R_s}{R} \frac{C_u}{C_g} \quad , \quad (54)$$

$$\sigma_m = Y \frac{1}{A} \frac{1}{k} \frac{1}{E} \frac{4}{n} \frac{C_u}{C_g} V_m \quad . \quad (55)$$

The second term of Eq. 51 cannot be incorporated into the calibration factor f. Therefore, it is provided here as reference for those who will be using the data provided by this instrumentation system.

Axial Stress Correction

As with the bending gauge circuits, the asymmetries of axial gauge placement produce cross talk between the various stress components. Rewriting Eq. 23 and including non-symmetric bending terms (see the derivation of Eq. 44) yields the following result for the measured axial stress $(\sigma)_m$:

$$(\sigma)_m = \sigma_a + \sigma_{fb} \frac{(y_2 + y_1)}{2\ y_m} + \sigma_{lb} \frac{(x_2 + x_1)}{2\ x_m} \quad , \quad (56)$$

where $(\sigma)_m$ is now the axial stress measured by the gauge circuit, and the other variables are defined above. The dimensions for the gauge placement are summarized in Tables II, III and IV. This formulation assumes that the axial stress is constant across the cross section.

<u>**Flatwise Axial**</u>: For a flatwise axial circuit, the gauges are placed symmetrically about the flatwise axis but not about the lead-lag axis; i.e., $y_2 = -y_1 = y_m$ and $x_1 = x_2$, with x_1 and x_2 positive. Rewriting Eq. 56 yields

$$(\sigma_{fa})_m = \sigma_{fa} + \sigma_{fb} \frac{(y_m - y_m)}{2\ y_m} + \sigma_{lb} \frac{(x_2 + x_1)}{2\ x_m} \quad , (57)$$

$$(\sigma_{fa})_m = \sigma_{fa} + \sigma_{lb} \frac{|x_2| + |x_1|}{2\ x_m} = \sigma_{fa} + \sigma_{lb} \frac{x_{av}}{x_m} \quad , (58)$$

or solving for σ_{fa}

$$\sigma_{fa} = (\sigma_{fa})_m - C_{fal}\ \sigma_{lb} \quad , (59)$$

where

$$C_{fal} = \frac{x_{av}}{x_m} \quad , (60)$$

The positive sign in the second term of Eq. 58 is shown to emphasize that a positive lead-lag bending moment will increase the measured flatwise axial strain and to permit the definition of the positive correction factor C_{fal}. This coefficient is listed in Table V.

<u>**Lead-Lag Axial**</u>: For a lead-lag axial circuit, the gauges are not symmetrical about either axis. In particular, $|x_2| > |x_1|$ with $x_1 < 0$ and $x_2 > 0$, and $|y_2| < |y_1|$ with both y_1 and y_2 negative. Rewriting Eq. 54 yields

$$(\sigma_{la})_m = \sigma_{la} - \sigma_{fb} \frac{|y_2| + |y_1|}{2\ y_m} - \sigma_{lb} \frac{|x_2| - |x_1|}{2\ x_m} \quad , (61)$$

$$(\sigma_{la})_m = \sigma_{la} - \sigma_{fb} \frac{y_{av}}{y_m} - \sigma_{lb} \frac{|\delta x|}{x_m} \quad , (62)$$

or

$$\sigma_{la} = (\sigma_{la})_m + C_{laf}\ \sigma_{fb} + C_{lal}\ \sigma_{lb} \quad , (63)$$

where

$$C_{laf} = \frac{y_{av}}{y_m} \qquad C_{lal} = \frac{|\delta x|}{x_m} \quad . (64)$$

The negative signs for the second and third terms in Eq. 61 are shown to emphasize that both positive flatwise and lead-lag bending moments will decrease the measured flatwise axial strain and to permit the definition of positive correction factors, Eq. 62. These two coefficients are listed in Table V.

Torque Gauges

The torque bridge uses four active elements, each set at ±45° to the axis of the shaft. Gauges B and D are oriented at +45° to the centerline of the shaft; and gauges A and C at

-45°. Gauges C and D are located on one side of the shaft; and A and C are located on the other; i.e., 180° around the shaft from each other.[4]

In this configuration, the shear stress in the outside fibers of the shaft, υ, is given by[5]

$$\upsilon = G\,(2\,\varepsilon) = \frac{Y}{1+\mu}\,\varepsilon \quad , \quad (65)$$

where μ is Possion's ratio. Performing the same analysis as cited in Eqs. 32 through 37 and Eq. 52 yields

$$f = \frac{Y}{1+\mu}\,\frac{1}{A}\,\frac{1}{k}\,\frac{1}{E}\,\frac{4}{n}\,\frac{1}{C_v}\,\frac{C_u}{C_g} \quad . \quad (66)$$

Similar analysis will yield expressions equivalent to Eqs. 40 and 41.

The output of this circuit is the shear stress in the shaft under consideration. To change the shear stress to torque requires a knowledge of the section properties of the shaft.

In particular, υ is related to the torque T in a circular shaft by

$$\upsilon = \frac{T\,D_o}{2\,I_P} \quad , \quad (67)$$

where I_P is the polar moment of inertia and D_o is the outside diameter of the shaft. For a hollow cylinder with an inside diameter of D_i and and outside diameter of D_o, I_P is given by

$$I_P = \frac{\pi}{32}\,(D_o^4 - D_i^4) \quad . \quad (68)$$

One should note that the combination of Eqs. 65, 67 and 68 leads to the direct determination of the torque in the shaft. However, because the determination of I_P is particularly susceptible to errors, the preferred method for determining a calibration factor for the torque is by direct calibration of the circuit by a known torque.

Gauge Installation

The gauges were installed by HiTec Corporation[6] using standard strain gauge installation techniques. The color codes for wiring these circuits are listed in Fig. 3 and summarized in Table VI.

All of the gauges were installed with M-Bond AE-10 epoxy.[2] A vacuum technique was used to degas the bond and to apply uniform pressure to the gauges during the bonding process.

Table VI. Color Codes for the Strain Gauge Circuits

Circuit Descriptor	Color Code
+ Excitation	Red
- Excitation	Black
+ Signal	Green
- Signal	White

After bonding and completing the electrical connections, the gauges and their respective completion units were coated with either M-Coat A[2] or M-Coat D[2] to provide an environmental seal. On the tower, epoxy was used to stabilize both the gauges and their circuits.

For the blade circuits, all gauges and completion units were sealed with M-Coat D[2]. As the blade circuits had to be smoothed into the contour of the blade section with a minimal effect on the flow field, the entire installation was covered with Hysol EA-960F Fast Room Temperature Curing Adhesive.[7] This compound was chosen for this application because it is a structural aerodynamic smoothing compound with effective barrier qualities and structural strength, and it is easy to sand. Each circuit was first coated with a light, red layer of the EA-960F and then a layer of blue EA-960F. The EA-960F covering was then faired into the blade contour by sanding. The two colored layers of EA-960F were used to protect the gauge circuits during the sanding process. In particular, if the red layer became visible during sanding, the sanding was stopped, more blue was applied and the fairing process was started over.

Strain Gauge Cables

The cables that were used to connect the gauges to the signal junction box are summarized in Appendices I through M. All cable types are specified by their Alpha[8] catalog number.

<u>Strain Gauge Cable Descriptors</u>: All of the strain gauge cables have been designated by the name of the strain gauge circuits they carry. As each cable carries only those signals from one section, the cables are designated by the first two letters of the strain gauge descriptors at that gauge section (see the section entitled Strain Gauge Descriptors); i.e., the key to the nomenclature used in this system is as follows:

First Letter or Number (see Fig. 2):
- 1 : Blade 1
- 2 : Blade 2
- T : Tower/Shaft
- B : Brake

Second Letter or Number (see Fig. 2):
- A through U, and X : Gauge Section
- N, S, E or W : Brake Location

Cable Routes: The strain gauge cables were all run through the longitudinal channels near the rear of the blade section, see Fig. 4. The cable for each gauge section was brought up through the blade using a "riser." A cable clamp that was screwed onto the riser provided a mechanical connection between the riser and the cable. The riser assembly was then potted in place using Hysol EA-934NA Room Temperature Curing Adhesive.[7] The two-colored fairing technique with Hysol EA-960F was used to fair the cable risers into the contour of the airfoil.

Lead Loss: The equations cited above assume that the excitation voltage E is measured at the connections of the Wheatstone Bridge. As this is not possible in our configuration, the supply voltage must be corrected for lead loss. If E is the voltage at the bridge, and E_s is the measured voltage at a lead distance L from the bridge, then

$$E = E_s \frac{R}{R + R_L} \quad , (69)$$

where

$$R_L = 2 \eta L \quad , (70)$$

where η is the resistance of the cable per unit length. The values for L are listed in Appendices P and Q. The value of η is a function of the wire used in the cable. For the 22-gauge cable used here, η equals 16.14 Ω per 1000 feet[9].

Completion Units

Preliminary tests revealed that a coating of EA-960F directly on the completion units could affect the output of the gauge circuits. The completion units were protected by placing a metal cover over them and then covering them with the Hysol EA-960F. This cover insured that an air gap (approximately one quarter of an inch) existed between the top of the completion unit and the EA-960F. The active strain gauges were covered with relatively thin layers of the EA-960F compound. To insure that this coating did not effect gauge performance, all blade sections were tested in 4-point bending, both before and after the EA-960F was applied. These experiments[10] showed that the output of the gauges was not affected by the EA-960F coating.

Lotus Files

All of the information cited in the appendices for the strain gauges have been programmed into a LOTUS[11] file entitled TBINST.WK1. This file and others describing the Test Bed instrumentation and configuration are maintained on the Test Bed site PC computer.

The calibration equations, Eqs. 31 through 68 have also been programmed in a LOTUS[11] file entitled TBCALF.WK1. The output of this file is summarized in Appendices I through L. This file uses the information contained in Appendices E through H for the gauge circuits, the lead lengths described in Appendices P and Q, the geometric correction terms defined in Table V, and the typical parameters cited above. Summarizing these parameters: A = 250; E_s = 10 v; n = 1, 2, or 4; C_v = 2000 counts/volt; C_u=6.894757E-3 Mpa/psi; R_s = 120 KΩ; V_m = ± 5 v; and η = 0.01614 Ω/ft. The material properties of aluminum are taken to be Y = 1E7 psi and μ = 0.316, and the properties of steel are taken to be Y = 3E7 psi and μ = 0.25.

DAMAGE GAUGES

To examine the fatigue damage accumulated in the blades, five damage gauges,[12] Fig. 5, were installed on Blade 2. Each damage gauge consists of a precracked aluminum coupon instrumented with a strain gauge and a KRAK gauge[13]. The strain gauge mounted on the damage coupon was given the designation xxF1 and the KRAK gauge designation is xxF2 (see Table VII and Appendix B).

The damage coupons were glued into place using Hysol EA934NA Room Temperature Curing Adhesive.[7] The coupon was held off of the blade using an aluminum shim. The height of the damage coupon (from the blade to the top surface of the coupon) is given in Table VII.

Again, the two-colored Hysol EA-960F fairing technique, with a metal cover for the gauge, was used to fair these gauges into the airfoil section.

PRESSURE LINES

To facilitate future research needs, six pressure lines were plumbed to the lower two kinks on Blade 2. Three sixteenth-inch copper tubing was used for each line. The rated working pressure for this tubing is 2000 psi. The tubing was routed through the third longitudinal channel (from the rear), see Fig. 4, of the lower 42-inch and 48-inch blade sections of

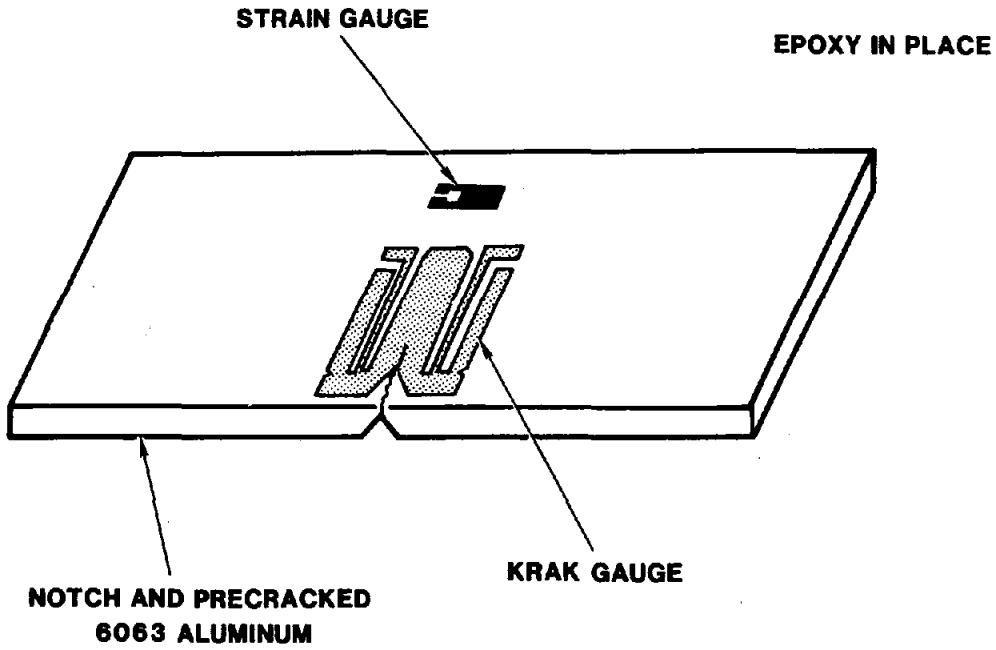

Figure 5. Schematic Diagram of the Damage Gauges

Table VII. Dimensions for the Damage Gauges

Damage Gauge	Height Dimension (in)	Average Bond Thickness (in)	Initial Crack Length (in)	
			In the Gauge	Total Length
2HF2	0.0735	0.003	0.110	0.410
2JF2*	0.0700	0.001	0.100	0.227
2LF2	0.0700	0.001	0.120	0.360
2NF2	0.0715	0.002	0.180	0.320
2QF2	0.0775	0.005	0.090	0.300

*This specimen was subjected to an over stress during the formation of the fatigue crack.

Blade 2 (the cables and the pipes are in different channels). Stainless steel risers were used to access the lines from the outside of the blade. Each riser was terminated with a union and cap at the outside blade surface.

The lower ends of the pressure lines are terminated with caps at the inside bottom of the tower.

AUXILIARY CABLES

In addition to the cables described above, 18 auxiliary signal cables and eight DAAS cables were plumbed about the rotor. All of the signal cables are brought to the signal junction box that is located inside the base of the tower. There are three classes of signal cables: data cables, power cables, and video cables. The DAAS cables connect the signal junction box to the PCM of the DAAS.[1]

Data Cables

A total of 14 auxiliary signal cables, summarized in Appendices R, S and T, were routed about the rotor. All cable types are specified by their Alpha[8] catalog number.

<u>Data Cable Descriptors</u>: All data cables were designated by their position. The key to the nomenclature used in this system is as follows (see the section entitled Strain Gauge Designators):

First Letter or Number (see Figs. 2 and 6):
- 1 : Blade 1
- 2 : Blade 2
- T : Tower/Shaft

Second Letter or Number (see Fig. 6):
- A through U, and X : Gauge Section

1, 2, 3, 4 or 5 : Kink Number
Additional Letters:
A : Accelerometer Cable
P1 : Pressure Tap Cable
P2 : Pressure Tap Cable

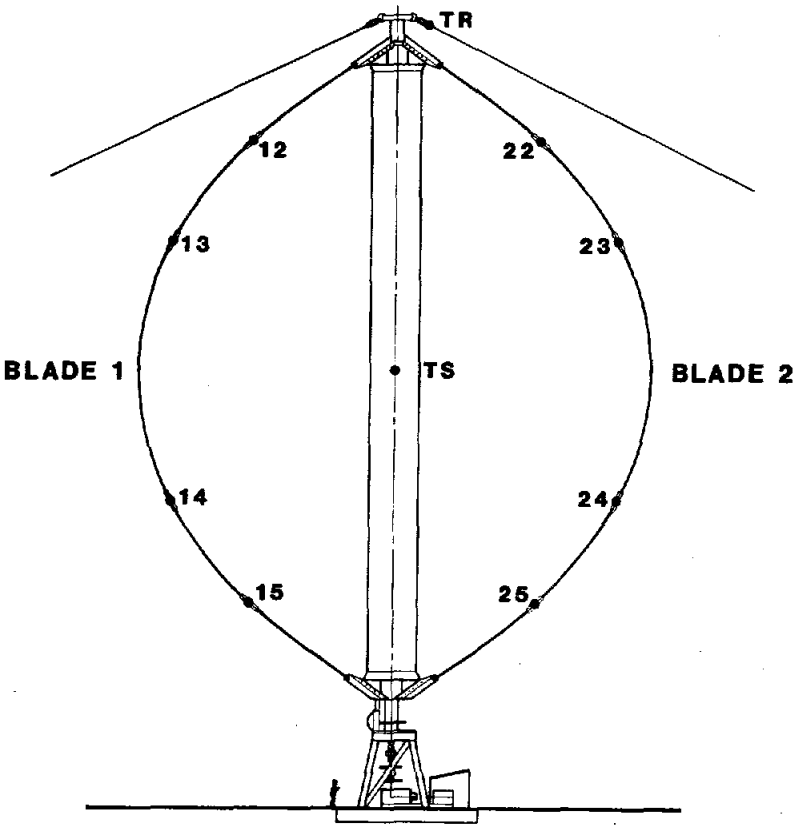

Figure 6. Nomenclature for the Accelerometer and Pressure Tap Cables

<u>A Cables</u>: An "xxA" cable was plumbed to each kink and to two positions on the tower, see Fig. 6. Each of these 10 cables contains 15 individually shielded, twisted pairs and is terminated on the rotor with an MS3100E 28-21P connector.[14] The other end of the cable was "pigtailed" in the bottom, inside of the tower near the signal junction box.

<u>P Cables</u>: An "xxP1" cable and an "xxP2" cable were plumbed to the bottom two "kinks" on Blade 1. Each of these four cables contained 19 individually shielded, twisted pairs and were terminated on the rotor with an MS3100E 28-21P connector.[14] The other end of the cable was "pigtailed" in the bottom, inside of the tower near the signal junction box.

Power Cables

Two power cables were plumbed to the top and middle of the tower, see Table VIII, Fig. 6, and Appendix R. These cables were labeled xxP, see the definitions for the first two descriptors listed above. Each of these cables was designed to carry 110 V ac power. During the construction of the tower, it was noted that these cables had been run parallel to all of the instrumentation cables. As this routing could create a noise problem in the data lines, two new cables were run inside metal conduit to the specified locations. The original wiring was disconnected, but left in place. Each of the two new cables was connected to the 110 V supply inside the tower.

Video Cables

Two video cables were plumbed to the top and middle of the tower, see Table VIII, Fig. 6 and Appendix R. These cables were labeled xxV, see the definitions for the first two descriptors listed above. Each of these cables was designed to carry video signals. Each of these two cables was terminated on the rotor with a BNC connector. The other end of the cable was "pigtailed" in the bottom, inside of the tower near the signal junction box.

Table VIII. Power and Video Cables

Cable Description	Approximate Position
TRP	Top of Tower
TRV	Top of Tower
TSP	Middle of Tower
TSV	Middle of Tower

SIGNAL JUNCTION BOX

As discussed above, the signal cables are connected to the DAAS in the signal junction box. The Signal Junction Box is made up of two Hoffman Screw Cover Enclosures[15] (Catalog Number A-301606LP) connected by two 3-inch conduits. The layout of the terminal blocks is shown in Fig. 7. The horizontal format blocks, across the top of box, are the connections to the DAAS, and the vertical format blocks are the connections to the gauges.

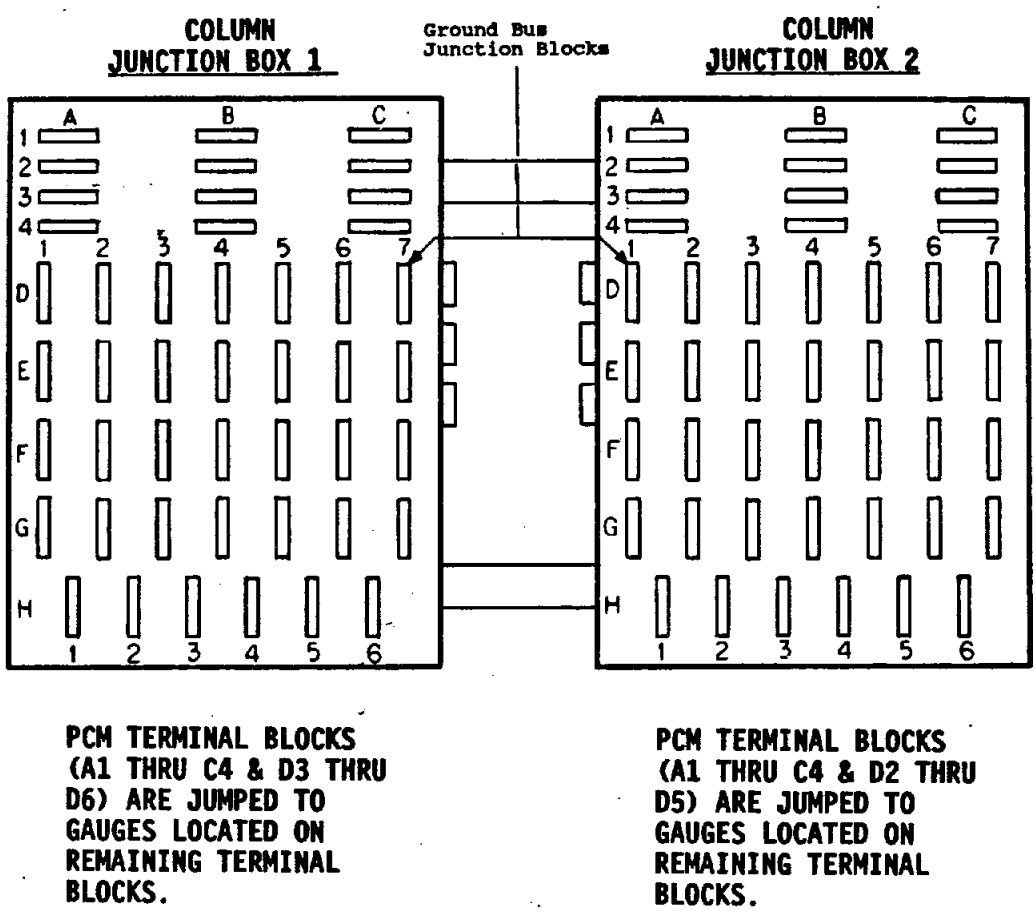

Figure 7. Terminal Block Locations in the Signal Junction Box

To insure that the gauge/instrumentation system did not contain ground loops, the ground connections (and/or shields) were wired as shown in Fig. 8. All grounds are connected to a single point at the bottom inside of the tower. To connect a particular gauge to a particular DAAS channel, a jumper cable must be installed between the respective terminal sets shown in Fig. 8.

The gauge/DAAS connections that were initially (i.e., when the blades were installed on the machine) used for the Test Bed are listed in Appendices U and V.

DAAS CABLES

To connect the signal junction box to the DAAS[1] and to provide power for the PCM required two sets of four cables. The color codes and pin connections for these cables are listed in Appendices W, X, Y and Z. The power cables, Appendix W, are terminated with an MS 3126F12-3S connector. The signal cables, Appendices X, Y and Z, are terminated with an MS 3126F22-55S connector.[14]

FOAMING

As discussed above, the blade cables and the pressure tubing were routed through blade channels near the rear of the airfoil, see Fig. 4. To support these cables during the operation of the machine, the channels containing the wires or the tubing were foamed throughout using Insta-Foam polyurethane foam.[16]

The foam used has a density of 1.75 pounds per cubic foot. Tests conducted on aluminum tubes containing cables showed that the foam flowed completely around the wires during the foaming process and was a very effective technique for locking the cables in place.

The thermal stability of the aluminum, cable and foam system was checked by cycling samples between -2°F and 122°F. Three samples were first heated in a 122°F oven. They were allowed to stabilize for a minimum of 8 hours. Then, they were moved directly to a freezer for cooling to -2°F. After a minimum stabilization period of 8 hours, they were returned to the oven. Upon completion of 30 temperature cycles, the samples were sectioned and compared with control samples. A slight discoloration of the foam near the edges of the sample was noted; however, no mechanical degradation was found, and the cables were still locked in place by the foam.

CONCLUDING REMARKS

This report describes the instrumentation that was placed on the Sandia 34-m Test Bed Vertical Axis Wind Turbine. The intent of the report is to outline the instrumentation that was placed on the rotor of this machine and to describe the provisions for future instrumentation that were incorporated into the rotor instrumentation circuits. This report is intended to be a reference manual for the rotor instrumentation of the Test Bed.

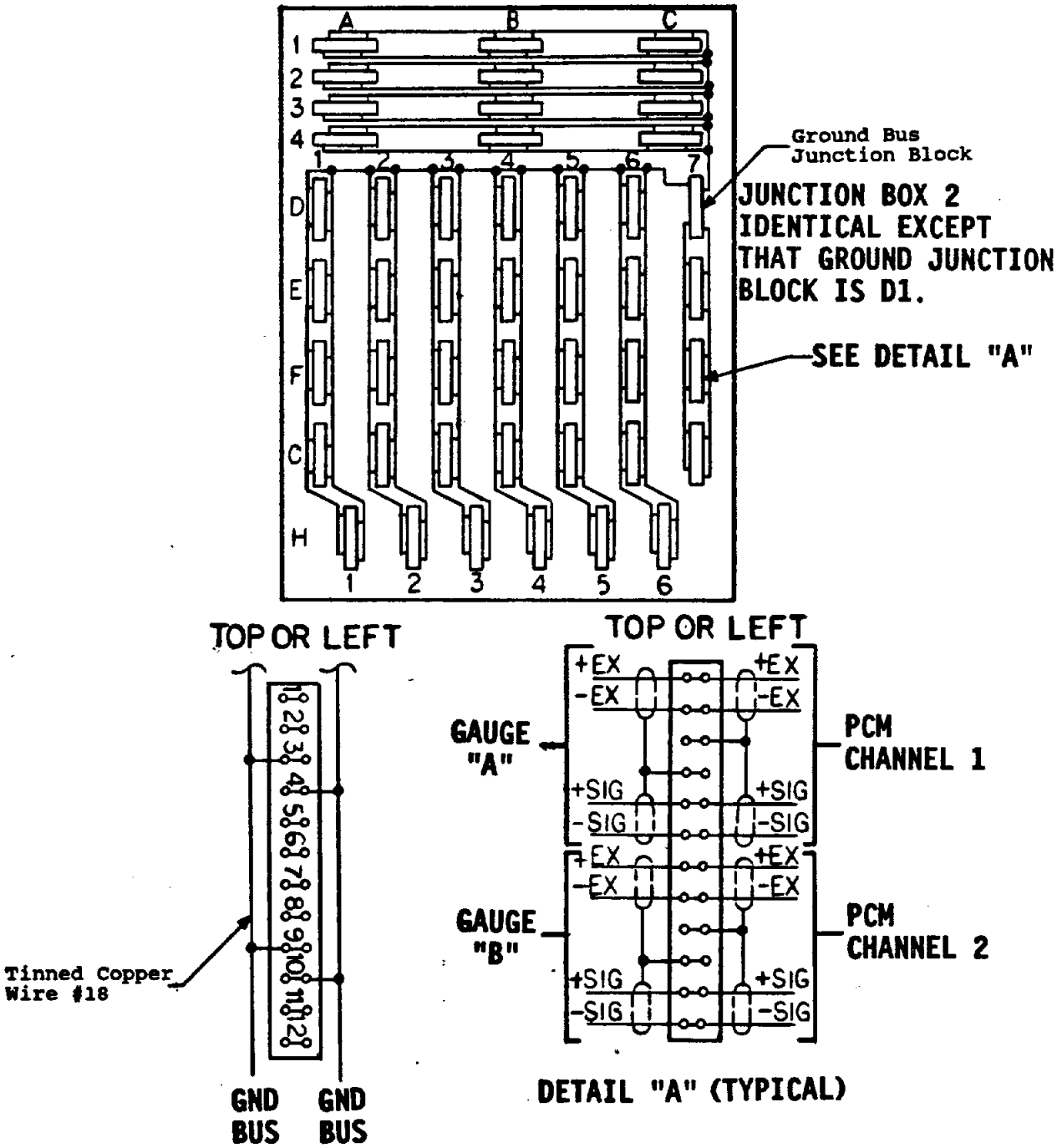

Figure 8. Ground Bus and Terminal Layout Plan for Signal Junction Box 1

The tables and appendices presented here were programmed on a computer at the Test Bed site. Lotus spreadsheet software[11] was used for it. As changes and additions are made to the system, the spreadsheet file can be modified easily to reflect these changes and provide current information for the setup of the rotor instrumentation.

REFERENCES

1. D. Berg, M. Rumsey, L. Gallo and D. Burwinkle, "Data Acquisition and Analysis System for the Sandia 34-Meter Vertical Axis Wind Turbine," *Proceedings of the Seventh ASME Wind Energy Symposium*, SED-Vol. 5, A. H. P. Swift and R. W. Thresher, eds., ASME, 1988, p. 53.

2. Micro-Measurements Division, Measurements Group, Inc., Raleigh, North Carolina 27611.

3. R. C. Dove and P. H. Adams, *Experimental Stress Analysis and Motion Measurement*, Merrill Books, Inc., Columbus, 1964.

4. J. Vaugham, *Strain Measurements*, Bruel & Kjaer, 1975.

5. W. M. Murray and P. K. Stein, *Lectures and Laboratory Exercises on Strain Gage Techniques*, Department of Engineering, University of California, August 18-29, 1958.

6. HiTec Corp., Nardone Industrial Park, Westford, MA 01886.

7. Hysol Division, The Dexter Corp., 2850 Willow Pass Rd., Pittsburg, CA 94565.

8. Alpha Wire Corp., 711 Liderwood Ave., PO Box 711, Elizabeth, NJ 07207-0711.

9. E. W. Schilling, *Electrical Engineering*, International Textbook Co., Scranton, 1960, p. 466.

10. H. J. Sutherland, *Strain Gauge Validation Experiments for the Sandia 34-Meter VAWT Test Bed*, SAND88-1807, Sandia National Laboratories, Albuquerque, NM 87185, in publication.

11. Lotus Development Corp., 55 Cambridge Parkway, Cambridge, MA 02142.

12. A. F. Grant, Jr. and A. Dumanis-Modan, *Evaluation of the Crack Growth Gage Concept as an Individual Aircraft Tracking Device*, Vol II, AFWAL-TR-83-3082, AFWAL/FIBEC, Wright-Patterson AFB, OH 45433, September 1983.

13. TTI Division, Hartrun Corp., 125 Columbia Court, Chaska, MI 55318.

14. Bendix, Electrical Components Division, Purchased through Hamilton Avnet Electronics, 350 McCormick Ave., Irvine Industrial Complex, Costa Mesa, CA 92626.

15. Hoffman Engineering Co., Division of Federal Cartridge Corp., Anoka, MI.

16. Insta-Foam Products, Inc., 1500 Cedarwood Drive, Jolliet IL 80435.

APPENDIX A.

Gauge Circuits for Blade 1

Gauge Desig	Approximate Position			Gauge Configuration
	Blade Section	Position* (in)	From	
1AML 1AMF	Upper 48	37.00 37.00	TOP	Lead-Lag Bending Flatwise Bending
1DML 1DMF	Upper 42	38.5 38.5	TOP	Lead-Lag Bending Flatwise Bending
1EML 1EMF	Upper 42	124.375 124.375	TOP	Lead-Lag Bending Flatwise Bending
1FML 1FMF	Upper 42	36.75 36.75	BOT	Lead-Lag Bending Flatwise Bending
1HML 1HMF 1HAF	Center 36	351.375 351.375 352.125	BOT	Lead-Lag Bending Flatwise Bending Flatwise Axial
1IML 1IMF	Center 36	36.75 36.75	BOT	Lead-Lag Bending Flatwise Bending
1LML 1LMF	Lower 42	123.0 123.0	BOT	Lead-Lag Bending Flatwise Bending
1NML 1NMF	Lower 42	36.0 36.0	BOT	Lead-Lag Bending Flatwise Bending
1OML 1OMF	Lower 48	36.625 36.625	TOP	Lead-Lag Bending Flatwise Bending
1PML 1PMF 1PAL 1PAF	Lower 48	121.25 121.25 121.25 121.25	BOT	Lead-Lag Bending Flatwise Bending Lead-Lag Axial Flatwise Axial
1QML 1QMF	Lower 48	36.0 36.0	BOT	Lead-Lag Bending Flatwise Bending

*The position cited here is the distance from the gauge to the top or bottom of the unreinforced blade section.

APPENDIX B.

Gauge Circuits for Blade 2

Gauge Desig	Approximate Position			Gauge Configuration
	Blade Section	Position (in)	From	
2XML 2XMF	Upper 48	36.0 36.0	TOP	Lead-Lag Bending Flatwise Bending
2AML 2AMF	Upper 48	245.75 245.75	TOP	Lead-Lag Bending Flatwise Bending
2DML 2DMF	Upper 42	37.0 37.0	TOP	Lead-Lag Bending Flatwise Bending
2GML 2GMF	Center 36	36.5 36.5	TOP	Lead-Lag Bending Flatwise Bending
2HML 2HMF 2HF1 2HF2	Center 36	351.375 351.375 351.375 351.375	TOP	Lead-Lag Bending Flatwise Bending Damage Axial Crack Length
2IML 2IMF 2IDF	Center 36	35.5 35.5 0.313	BOT	Lead-Lag Bending Flatwise Bending Flatwise Total
2JMF 2JF1 2JF2 2JDF	Lower 42	38.375 34.375 34.375 0.25	TOP	Flatwise Bending Damage Axial Crack Length Flatwise Total
2KMF	Lower 42	81.25	TOP	Flatwise Bending
2LMF 2LF1 2LF2	Lower 42	122.875 126.5 126.5	BOT	Flatwise Bending Damage Axial Crack Length
2MMF	Lower 42	79.625	BOT	Flatwise Bending
2NMF 2NF1 2NF2 2NDF 2NML	Lower 42	36.75 39.75 39.75 0.25 36.75	BOT	Flatwise Bending Damage Axial Crack Length Flatwise Total Lead-Lag Bending

APPENDIX B. (cont).

Gauge Desig	Approximate Position			Gauge Configuration
	Blade Section	Position* (in)	From	
2PMF	Lower 48	121.75	BOT	Flatwise Bending
2PAL		121.75		Lead-Lag Axial
2QDF1	Lower 48	0.375	BOT	Flatwise Total
2QDF2		6.0		Flatwise Total
2QDF3		17.625		Flatwise Total
2QDL		0.375		Lead-Lag Total
2QF1		6.0		Damage Axial
2QF2		6.0		Crack Length

APPENDIX C.

Gauge Circuits for the Tower

Gauge Desig	Approximate Position	Gauge Configuration
TSMI TSMO TSRA TSRB TSRC TSRT	Middle of Tower	In-Plane Bending Out-Plane Bending Vertical Strain 45° Strain Horizontal Strain Torque
TTMI TTMO	Bottom of Tower	In-Plane Bending Out-Plane Bending
TUAI TURA TURB TURC TURT	Middle of Low Speed Shaft	In-Plane Bending Vertical Strain 45° Strain Horizontal Strain Torque

APPENDIX D

Gauge Circuits for the Brakes

Brake Direc	Approximate Position	Gauge Desig
North South East West	Upper Arm	BNAU BSAU BEAU BWAU
North South East West	Lower Arm	BNAL BSAL BEAL BWAL

APPENDIX E.

Gauge Circuit Configurations and Gauge Factors for Blade 1

Gauge Desig	Bride Circuit	Gauge Factor	Active Elements	Gauge
1AML	Moment Pr	2.18	2	WK-13-250BG-350
1AMF	Moment Pr	2.18	2	WK-13-250BG-350
1DML	Moment Pr	2.18	2	WK-13-250BG-350
1DMF	Moment Pr	2.18	2	WK-13-250BG-350
1EML	Moment Pr	2.18	2	WK-13-250BG-350
1EMF	Moment Pr	2.18	2	WK-13-250BG-350
1FML	Moment Pr	2.18	2	WK-13-250BG-350
1FMF	Moment Pr	2.18	2	WK-13-250BG-350
1HML	Moment Pr	2.18	2	WK-13-250BG-350
1HMF	Moment Pr	2.18	2	WK-13-250BG-350
1HAF	Axial Pr	2.18	2	WK-13-250BG-350
1IML	Moment Pr	2.18	2	WK-13-250BG-350
1IMF	Moment Pr	2.18	2	WK-13-250BG-350
1LML	Moment Pr	2.18	2	WK-13-250BG-350
1LMF	Moment Pr	2.18	2	WK-13-250BG-350
1NML	Moment Pr	2.18	2	WK-13-250BG-350
1NMF	Moment Pr	2.18	2	WK-13-250BG-350
1OML	Moment Pr	2.18	2	WK-13-250BG-350
1OMF	Moment Pr	2.18	2	WK-13-250BG-350
1PML	Moment Pr	2.18	2	WK-13-250BG-350
1PMF	Moment Pr	2.18	2	WK-13-250BG-350
1PAL	Axial Pr	2.18	2	WK-13-250BG-350
1PAF	Axial Pr	2.18	2	WK-13-250BG-350
1QML	Moment Pr	2.18	2	WK-13-250BG-350
1QMF	Moment Pr	2.18	2	WK-13-250BG-350

APPENDIX F.

Gauge Circuit Configurations and Gauge Factors for Blade 2

Gauge Desig	Bridge Circuit	Gauge Factor	Active Elements	Gauge
2XML	Moment Pr	2.18	2	WK-13-250BG-350
2XMF	Moment Pr	2.18	2	WK-13-250BG-350
2AML	Moment Pr	2.18	2	WK-13-250BG-350
2AMF	Moment Pr	2.18	2	WK-13-250BG-350
2DML	Moment Pr	2.18	2	WK-13-250BG-350
2DMF	Moment Pr	2.18	2	WK-13-250BG-350
2GML	Moment Pr	2.18	2	WK-13-250BG-350
2GMF	Moment Pr	2.18	2	WK-13-250BG-350
2HML	Moment Pr	2.18	2	WK-13-250BG-350
2HMF	Moment Pr	2.18	2	WK-13-250BG-350
2HF1	Single	2.05	1	WK-13-062AP-350
2HF2	Krak	-	1	KG-A10
2IML	Moment Pr	2.18	2	WK-13-250BG-350
2IMF	Moment Pr	2.18	2	WK-13-250BG-350
2IDF	Single	2.18	1	WK-13-250BG-350
2JMF	Moment Pr	2.18	2	WK-13-250BG-350
2JF1	Single	2.05	1	WK-13-062AP-350
2JF2	Krak	-	1	KG-A10
2JDF	Single	2.18	1	WK-13-250BG-350
2KMF	Moment Pr	2.15	2	CEA-13-062UW-350
2LMF	Moment Pr	2.18	2	WK-13-250BG-350
2LF1	Single	2.05	1	WK-13-062AP-350
2LF2	Krack	-	1	KG-A10
2MMF	Moment Pr	2.15	2	CEA-13-062UW-350
2NMF	Moment Pr	2.18	2	WK-13-250BG-350
2NF1	Single	2.05	1	WK-13-062AP-350
2NF2	Krack	-	1	KG-A10
2NDF	Single	2.18	1	WK-13-250BG-350
2NML	Moment Pr	2.18	2	WK-13-250BG-350
2PMF	Moment Pr	2.18	2	WK-13-250BG-350
2PAL	Axial Pr	2.18	2	WK-13-250BG-350

APPENDIX F (cont).

Gauge Desig	Bridge Circuit	Gauge Factor	Active Elements	Gauge
2QDF1	Single	2.18	1	WK-13-250BG-350
2QDF2	Single	2.18	1	WK-13-250BG-350
2QDF3	Single	2.18	1	WK-13-250BG-350
2QDL	Single	2.18	1	WK-13-250BG-350
2QF1	Single	2.05	1	WK-13-062AP-350
2QF2	Krack	-	1	KG-A10

APPENDIX G.

Gauge Circuit Configurations and Gauge Factors for the Tower

Gauge Desig	Bridge Circuit	Gauge Factor	Active Elements	Gauge
TSMI	Moment Pr	2.18	2	WK-13-250BG-350
TSMO	Moment Pr	2.18	2	WK-13-250BG-350
TSRA	Triaxial	2.10	1	CEA-13-250UR-350
TSRB	Triaxial	2.125	1	CEA-13-250UR-350
TSRC	Triaxial	2.10	1	CEA-13-250UR-350
TSRT	Torque	2.075	4	CEA-13-187UV-350
TTMI	Moment Pr	2.18	2	WK-13-250BG-350
TTMO	Moment Pr	2.18	2	WK-13-250BG-350
TUAI	Moment Pr	2.05	2	WK-06-250BG-350
TURA	Triaxial	2.07	1	CEA-06-250UR-350
TURB	Triaxial	2.07	1	CEA-06-250UR-350
TURC	Triaxial	2.07	1	CEA-06-250UR-350
TURT	Torque	2.04	4	CEA-06-187UV-350

APPENDIX H.

Gauge Circuit Configurations and Gauge Factors for the Brakes

Gauge Desig	Bridge Circuit	Gauge Factor	Active Elements	Gauge
BNAU	Axial Pr	2.05	2	WK-06-250BG-350
BSAU	Axial Pr	2.05	2	WK-06-250BG-350
BEAU	Axial Pr	2.05	2	WK-06-250BG-350
BWAU	Axial Pr	2.05	2	WK-06-250BG-350
BNAL	Axial Pr	2.05	2	WK-06-250BG-350
BSAL	Axial Pr	2.05	2	WK-06-250BG-350
BEAL	Axial Pr	2.05	2	WK-06-250BG-350
BWAL	Axial Pr	2.05	2	WK-06-250BG-350

APPENDIX I.

Calibration Factors for Blade 1

Gauge Desig	Calibration Factor (Mpa/cnts)	Maximum Stress (Mpa)	Cal Stress (MPa)	Cal Strain (micro strain)	Cal Voltage (volt)
1AML	0.01428876	142.887	58.182	843.86	2.0359
1AMF	0.01290237	129.023	52.537	761.98	2.0359
1DML	0.01396109	139.610	56.676	822.02	2.0297
1DMF	0.01294146	129.414	52.537	761.98	2.0297
1EML	0.01396990	139.698	56.676	822.02	2.0285
1EMF	0.01294963	129.496	52.537	761.98	2.0285
1FML	0.01397808	139.780	56.676	822.02	2.0273
1FMF	0.01295721	129.572	52.537	761.98	2.0273
1HML	0.01377888	137.788	56.631	821.36	2.0549
1HMF	0.01278278	127.827	52.537	761.98	2.0549
1HAF	0.01278278	127.827	52.537	761.98	2.0549
1IML	0.01374493	137.449	56.631	821.36	2.0600
1IMF	0.01275127	127.512	52.537	761.98	2.0600
1LML	0.01374333	137.433	56.676	822.02	2.0619
1LMF	0.01273961	127.396	52.537	761.98	2.0619
1NML	0.01372193	137.219	56.676	822.02	2.0651
1NMF	0.01271977	127.197	52.537	761.98	2.0651
1OML	0.01404519	140.451	58.182	843.86	2.0712
1OMF	0.01268243	126.824	52.537	761.98	2.0712
1PML	0.01406328	140.632	58.182	843.86	2.0685
1PMF	0.01269877	126.987	52.537	761.98	2.0685
1PAL	0.01269877	126.987	52.537	761.98	2.0685
1PAF	0.01269877	126.987	52.537	761.98	2.0685
1QML	0.01405423	140.542	58.182	843.86	2.0699
1QMF	0.01269060	126.906	52.537	761.98	2.0699

APPENDIX J.

Calibration Factors for Blade 2

Gauge Desig	Calibration Factor (Mpa/cnts)	Max Stress (Mpa)	Cal Stress (MPa)	Cal Strain (micro strain)	Cal Voltage (volt)
2XML	0.01429457	142.945	58.182	843.86	2.0351
2XMF	0.01290762	129.076	52.537	761.98	2.0351
2AML	0.01430749	143.074	58.182	843.86	2.0332
2AMF	0.01291929	129.192	52.537	761.98	2.0332
2DML	0.01395479	139.547	56.676	822.02	2.0307
2DMF	0.01293562	129.356	52.537	761.98	2.0307
2GML	0.01398074	139.807	56.631	821.36	2.0253
2GMF	0.01297004	129.700	52.537	761.98	2.0253
2HML	0.01378014	137.801	56.631	821.36	2.0548
2HMF	0.01278394	127.839	52.537	761.98	2.0548
2HF1	0.02718926	271.892	111.73	1620.6	2.0548
2IML	0.01374807	137.480	56.631	821.36	2.0596
2IMF	0.01275419	127.541	52.537	761.98	2.0596
2IDF	0.02550838	255.083	105.07	1523.9	2.0596
2JMF	0.01273727	127.372	52.537	761.98	2.0623
2JF1	0.02709000	270.900	111.73	1620.6	2.0623
2JDF	0.02547454	254.745	105.07	1523.9	2.0623
2KMF	0.01291500	129.150	53.270	772.61	2.0623
2LMF	0.01273085	127.308	52.537	761.98	2.0633
2LF1	0.02707635	270.763	111.73	1620.6	2.0633
2MMF	0.01289607	128.960	53.270	772.61	2.0653

APPENDIX J (cont).

Gauge Desig	Calibration Factor (Mpa/cnts)	Max Stress (Mpa)	Cal Stress (MPa)	Cal Strain (micro strain)	Cal Voltage (volt)
2NMF	0.01272327	127.232	52.537	761.98	2.0646
2NF1	0.02706022	270.602	111.73	1620.6	2.0646
2NDF	0.02544654	254.465	105.07	1523.9	2.0646
2NML	0.01372571	137.257	56.676	822.02	2.0646
2PMF	0.01270810	127.081	52.537	761.98	2.0670
2PAL	0.01270810	127.081	52.537	761.98	2.0670
2QDF1	0.02538003	253.800	105.07	1523.9	2.0700
2QDF2	0.02538003	253.800	105.07	1523.9	2.0700
2QDF3	0.02538003	253.800	105.07	1523.9	2.0700
2QDL	0.02538003	253.800	105.07	1523.9	2.0700
2QF1	0.02698950	269.895	111.73	1620.6	2.0700

APPENDIX K.

Calibration Factors for the Tower

Gauge Desig	Calibration Factor (Mpa/cnts)	Max Stress (Mpa)	Cal Stress (MPa)	Cal Strain (micro strain)	Cal Voltage (volt)
TSMI	0.01281428	128.142	52.537	761.98	2.0499
TSMO	0.01281428	128.142	52.537	761.98	2.0499
TSRA	0.02660488	266.048	109.07	1582.0	2.0499
TSRB	0.02629189	262.918	107.79	1563.4	2.0499
TSRC	0.02660488	266.048	109.07	1582.0	2.0499
TSRT	0.00511501	51.1501	20.970	400.27	2.0499
TTMI	0.01268010	126.800	52.537	761.98	2.0716
TTMO	0.01268010	126.800	52.537	761.98	2.0716
TUAI	0.04045261	404.526	167.60	810.30	2.0716
TURA	0.08012353	801.235	331.97	1604.9	2.0716
TURB	0.08012353	801.235	331.97	1604.9	2.0716
TURC	0.08012353	801.235	331.97	1604.9	2.0716
TURT	0.01626036	162.603	67.371	407.13	2.0716

APPENDIX L.

Calibration Factors for the Brakes

Gauge Desig	Calibration Factor (Mpa/cnts)	Max Stress (Mpa)	Cal Stress (MPa)	Cal Strain (micro strain)	Cal Voltage (volt)
BNAU	0.04069456	406.945	167.60	810.30	2.0593
BSAU	0.04069456	406.945	167.60	810.30	2.0593
BEAU	0.04069456	406.945	167.60	810.30	2.0593
BWAU	0.04069456	406.945	167.60	810.30	2.0593
BNAL	0.04069456	406.945	167.60	810.30	2.0593
BSAL	0.04069456	406.945	167.60	810.30	2.0593
BEAL	0.04069456	406.945	167.60	810.30	2.0593
BWAL	0.04069456	406.945	167.60	810.30	2.0593

APPENDIX M.

Color Codes for Blade 1 Cables

Cable Desig	Gauge Desig	Pair 1		Pair 2	
		+Pow	-Pow	+Sig	-Sig
1A	1AML	BLK	RED	BLK	WH
	1AMF	BLK	GRN	BLK	BLU
1D	1DML	BLK	RED	BLK	WH
	1DMF	BLK	GRN	BLK	BLU
1E	1EML	BLK	RED	BLK	WH
	1EMF	BLK	GRN	BLK	BLU
1F	1FML	BLK	RED	BLK	WH
	1FMF	BLK	GRN	BLK	BLU
1H	1HML	BLK	RED	BLK	WH
	1HMF	BLK	GRN	BLK	BLU
	1HAF	BLK	BRN	BLK	YEL
1I	1IML	BLK	RED	BLK	WH
	1IMF	BLK	GRN	BLK	BLU
1L	1LML	BLK	RED	BLK	WH
	1LMF	BLK	GRN	BLK	BLU
1N	1NML	BLK	RED	BLK	WH
	1NMF	BLK	GRN	BLK	BLU
1O	1OML	BLK	RED	BLK	WH
	1OMF	BLK	GRN	BLK	BLU
1P	1PML	BLK	RED	BLK	WH
	1PMF	BLK	GRN	BLK	BLU
	1PAL	BLK	BRN	BLK	YEL
	1PAF	BLK	ORG	RED	GRN
1Q	1QML	BLK	RED	BLK	WH
	1QMF	BLK	GRN	BLK	BLU

APPENDIX N.

Color Codes for Blade 2 Cables

Cable Desig	Gauge Desig	Pair 1		Pair 2	
		+Pow	-Pow	+Sig	-Sig
2X	2XML	BLK	RED	BLK	WH
	2XMF	BLK	GRN	BLK	BLU
2A	2AML	BLK	RED	BLK	WH
	2AMF	BLK	GRN	BLK	BLU
2D	2DML	BLK	RED	BLK	WH
	2DMF	BLK	GRN	BLK	BLU
2G	2GML	BLK	RED	BLK	WH
	2GMF	BLK	GRN	BLK	BLU
2H	2HML	BLK	RED	BLK	WH
	2HMF	BLK	GRN	BLK	BLU
	2HF1	BLK	BRN	BLK	YEL
	2HF2	BLK	ORG	RED	GRN
2I	2IML	BLK	RED	BLK	WH
	2IMF	BLK	GRN	BLK	BLU
	2IDF	BLK	BRN	BLK	YEL
2J	2JMF	BLK	RED	BLK	WH
	2JF1	BLK	GRN	BLK	BLU
	2JF2	BLK	BRN	BLK	YEL
	2JDF	BLK	ORG	RED	GRN
2K	2KMF	BLK	RED	BLK	WH
2L	2LMF	BLK	RED	BLK	WH
	2LF1	BLK	GRN	BLK	BLU
	2LF2	BLK	BRN	BLK	YEL
2M	2MMF	BLK	RED	BLK	WH
2N	2NMF	BLK	RED	BLK	WH
	2NF1	BLK	GRN	BLK	BLU
	2NF2	BLK	BRN	BLK	YEL
	2NDF	BLK	ORG	RED	GRN
	2NML	RED	WH	RED	BLU
2P	2PMF	BLK	RED	BLK	WH
	2PAL	BLK	GRN	BLK	BLU

APPENDIX N (cont).

Cable Desig	Gauge Desig	Pair 1		Pair 2	
		+Pow	-Pow	+Sig	-Sig
2Q	2QDF1	BLK	RED	BLK	WH
	2QDF2	BLK	GRN	BLK	BLU
	2QDF3	BLK	BRN	BLK	YEL
	2QDF	BLK	ORG	RED	GRN
	2QF1	RED	WH	RED	BLU
	2QF2	RED	YEL	RED	BRN

APPENDIX O.

Color Codes for the Tower Cables

Cable Desig	Gauge Desig	Pair 1		Pair 2	
		+Pow	-Pow	+Sig	-Sig
TS	TSMI	BLK	RED	BLK	WH
	TSMO	BLK	GRN	BLK	BLU
	TSRA	BLK	BRN	BLK	YEL
	TSRB	BLK	ORG	RED	GRN
	TSRC	RED	WH	RED	BLU
	TSRT	RED	YEL	RED	BRN
TT	TTMI	BLK	RED	BLK	WH
	TTMO	BLK	GRN	BLK	BLU
TU	TUAI	BLK	RED	BLK	WH
	TURA	BLK	GRN	BLK	BLU
	TURB	BLK	BRN	BLK	YEL
	TURC	BLK	ORG	RED	GRN
	TURT	RED	WH	RED	BLU

APPENDIX P.

Blade Cable Lengths and Types

Blade	Cable Designation	Cable Length (ft)	Cable Type	Twist Pairs	Weight (lbs/ft)
1	1A	215.5	6012	6	0.088
1	1D	249.0	6012	6	0.088
1	1E	256.0	6012	6	0.088
1	1F	262.5	6012	6	0.088
1	1H	113.0	6012	6	0.088
1	1I	86.0	6012	6	0.088
1	1L	76.0	6012	6	0.088
1	1N	59.0	6012	6	0.088
1	1O	27.0	6012	6	0.088
1	1P	41.0	6014	9	0.125
1	1Q	34.0	6012	6	0.088
2	2X	40.* 180.**	6012 6018	6 15	0.088 0.188
2	2A	230.0	6012	6	0.088
2	2D	244.0	6012	6	0.088
2	2G	273.5	6012	6	0.088
2	2H	114.0	6014	9	0.125

* Run inside of blade 2.
**Run down the tower to the Signal Junction Box.

APPENDIX P (cont).

Blade	Cable Designation	Cable Length (ft)	Cable Type	Twist Pairs	Weight (lbs/ft)
2	2I	88.5	6012	6	0.088
2	2J	74.0	6014	9	0.125
2	2K	74.0	6012	6	0.088
2	2L	68.5	6012	6	0.088
2	2M	58.0	6010	3	0.048
2	2N	62.0	6018	15	0.188
2	2P	49.0	6012	6	0.088
2	2Q	33.5	6018	15	0.188

APPENDIX Q.

Tower Cable Lengths and Types

Cable Designation	Cable Length (ft)	Cable Type	Twist Pairs	Weight (lbs/ft)
TS	140	6018	15	0.188
TT	25	6012	6	0.088
TU	25	6016	11	0.140

APPENDIX R.

Auxilary Cable Lengths and Types

Cable Designation	Cable Length (ft)	Cable Type	Twist Pairs	Weight (lbs/ft)
12A	238.0	6018	15	0.188
13A	266.5	6018	15	0.188
14A	78.0	6018	15	0.188
15A	56.0	6018	15	0.188
22A	235.5	6018	15	0.188
23A	240.0	6018	15	0.188
24A	80.0	6018	15	0.188
25A	52.0	6018	15	0.188
14P1	80.0	6020	19	0.255
14P2	79.0	6020	19	0.255
15P1	51.0	6020	19	0.255
15P2	48.0	6020	19	0.255
TRA	230.0	6018	15	0.188
TRV	230.0	RG-58	1	-
TRP	230.0	1401	3	-
TSA	120.0	6018	15	0.188
TSV	120.0	RG-58	1	-
TSP	120.0	1401	3	-

APPENDIX S.

Color Codes and Pin Connections for Cables 12A, 13A, 14A, 15A, 22A, 23A, 24A, 25A, TRA AND TSA

PAIR NO	PIN NO	COLOR CODE
1	A	BLK
	B	RED
2	C	BLK
	D	WHT
3	E	BLK
	F	GRN
4	G	BLK
	H	BLU
5	K	BLK
	L	BRN
6	M	BLK
	N	YEL
7	P	BLK
	R	ORG
8	S	RED
	T	GRN

PAIR 33 NO	PIN 33 NO	COLOR 33 CODE
9	U	RED
	V	WHT
10	W	RED
	X	BLU
11	a	RED
	b	YEL
12	c	RED
	d	BRN
13	e	RED
	f	ORG
14	g	GRN
	h	BLU
15	j	GRN
	k	WHT

APPENDIX T.

Color Codes and Pin Connections for the Cables 14P1, 14P2, 15P1 and 15P2

PAIR NO	PIN NO	COLOR CODE
1	A	BLK
	B	RED
2	C	BLK
	D	WHT
3	E	BLK
	F	GRN
4	G	BLK
	H	BLU
5	K	BLK
	L	BRN
6	M	BLK
	N	YEL
7	P	BLK
	J	ORG
8	S	RED
	T	GRN
9	U	RED
	V	WHT
10	W	RED
	X	BLU

PAIR NO	PIN NO	COLOR CODE
11	R	RED
	Z	YEL
12	a	RED
	b	BRN
13	c	RED
	d	ORG
14	e	GRN
	f	BLU
15	g	GRN
	h	WHT
16	j	GRN
	k	BRN
17	n	GRN
	p	ORG
18	r	GRN
	s	YEL
19	m	WHT
	*	BLU

* Extra Wire in the Cable.

APPENDIX U.

Initial Layout of the Gauges in the Signal Junction Box

PCM-1 CHAN	PCM-1 CABLE	PCM TERM & JBOX	GAUG TERM & JBOX	GAUG DESI	PAIR		PAIR	
					+EXT	-EXT	+SIG	-SIG
1	J-2	A1-1	F1-1	1AML	BLK	RED	BLK	WH
2	J-2	A1-1	F1-1	1AMF	BLK	GRN	BLK	BLU
3	J-2	B1-1	F2-1	1DMF	BLK	GRN	BLK	BLU
4	J-2	B1-1	F3-1	1EML	BLK	RED	BLK	WHT
5	J-2	C1-1	F3-1	1EMF	BLK	GRN	BLK	BLU
6	J-2	C1-1	F4-1	1FMF	BLK	GRN	BLK	BLU
7	J-2	A2-1	E1-2	1HML	BLK	RED	BLK	WHT
8	J-2	A2-1	E1-2	1HMF	BLK	GRN	BLK	BLU
9	J-2	B2-1	E2-2	1HAF	BLK	BRN	BLK	YEL
10	J-2	B2-1	E3-2	1IMF	BLK	GRN	BLK	BLU
11	J-2	C2-1	E4-2	1LML	BLK	RED	BLK	WHT
12	J-2	C2-1	E4-2	1LMF	BLK	GRN	BLK	BLU
13	J-3	A3-1	D2-1	TSMI	BLK	RED	BLK	WHT
14	J-3	A3-1	D2-1	TSMO	BLK	GRN	BLK	BLU
15	J-3	B3-1	E5-2	1NMF	BLK	GRN	BLK	BLU
16	J-3	B3-1	E6-2	1OMF	BLK	GRN	BLK	BLU

APPENDIX U (cont).

PCM-1 CHAN	PCM-1 CABLE	PCM TERM & JBOX	GAUG TERM & JBOX	GAUG DESI	PAIR		PAIR	
					+EXT	-EXT	+SIG	-SIG
17	J-3	C3-1	E7-2	1PMF	BLK	GRN	BLK	BLU
18	J-3	C3-1	F1-2	1PAL	BLK	BRN	BLK	YEL
19	J-3	A4-1	F1-2	1PAF	BLK	ORG	RED	GRN
20	J-3	A4-1	F2-2	1QML	BLK	RED	BLK	WHT
21	J-3	B4-1	F2-2	1QMF	BLK	GRN	BLK	BLU
22	J-3	B4-1	F5-2	2XML	BLK	RED	BLK	WHT
23	J-3	C4-1	F5-2	2XMF	BLK	GRN	BLK	BLU
24	J-3	C4-1	F3-2	2HMF	BLK	GRN	BLK	BLU
25	J-4	D3-1	E5-1	TURT	RED	WHT	RED	BLU
26	J-4	D3-1	F6-2	2IDF	BLK	BRN	BLK	YEL
27	J-4	D4-1	G6-2	2NDF	BLK	ORG	RED	GRN
28	J-4	D4-1	H1-2	2QDF	BLK	RED	BLK	WHT
29	J-4	D5-1	H1-2	2QDF	BLK	GRN	BLK	BLU
30	J-4	D5-1	H2-2	2QDF	BLK	BRN	BLK	YEL
31	J-4	D6-1		0 RE				
32	J-4	D6-1		4.1				

APPENDIX V.

Initial Layout of the Jumper Cables in the Signal Junction Box

JUNC BOX	TERM BLOCK	GAUGE OR CHAN DESIG	PAIR 1		PAIR 2	
			+EXT	-EXT	+SIG	-SIG
1	F1	1AML	BLK	RED	BLK	WH
1	F1	1AMF	BLK	GRN	BLK	BLU
1	F2	1DML	BLK	RED	BLK	WH
1	F2	1DMF	BLK	GRN	BLK	BLU
1	F3	1EML	BLK	RED	BLK	WH
1	F3	1EMF	BLK	GRN	BLK	BLU
1	F4	1FML	BLK	RED	BLK	WH
1	F4	1FMF	BLK	GRN	BLK	BLU
2	E1	1HML	BLK	RED	BLK	WH
2	E1	1HMF	BLK	GRN	BLK	BLU
2	E2	1HAF	BLK	BRN	BLK	YEL
2	E3	1IML	BLK	RED	BLK	WH
2	E3	1IMF	BLK	GRN	BLK	BLU
2	E4	1LML	BLK	RED	BLK	WH
2	E4	1LMF	BLK	GRN	BLK	BLU
2	E5	1NML	BLK	RED	BLK	WH
2	E5	1NMF	BLK	GRN	BLK	BLU

APPENDIX V (cont).

JUNC BOX	TERM BLOCK	GAUGE OR CHAN DESIG	PAIR 1		PAIR 2	
			+EXT	-EXT	+SIG	-SIG
2	E6	1OML	BLK	RED	BLK	WH
2	E6	1OMF	BLK	GRN	BLK	BLU
2	E7	1PML	BLK	RED	BLK	WH
2	E7	1PMF	BLK	GRN	BLK	BLU
2	F1	1PAL	BLK	BRN	BLK	YEL
2	F1	1PAF	BLK	ORG	RED	GRN
2	F2	1QML	BLK	RED	BLK	WH
2	F2	1QMF	BLK	GRN	BLK	BLU
2	F5	2XML	BLK	RED	BLK	WH
2	F5	2XMF	BLK	GRN	BLK	BLU
2	F6	2AML	BLK	RED	BLK	WH
2	F6	2AMF	BLK	GRN	BLK	BLU
1	F7	2DML	BLK	RED	BLK	WH
1	F7	2DMF	BLK	GRN	BLK	BLU
1	G1	2GML	BLK	RED	BLK	WH
1	G1	2GMF	BLK	GRN	BLK	BLU

APPENDIX V (cont).

JUNC BOX	TERM BLOCK	GAUGE OR CHAN DESIG	PAIR 1		PAIR 2	
			+EXT	-EXT	+SIG	-SIG
2	F3	2HML	BLK	RED	BLK	WH
2	F3	2HMF	BLK	GRN	BLK	BLU
2	F4	2HF1	BLK	BRN	BLK	YEL
2	F4	2HF2	BLK	ORG	RED	GRN
2	F5	2IML	BLK	RED	BLK	WH
2	F5	2IMF	BLK	GRN	BLK	BLU
2	F6	2IDF	BLK	BRN	BLK	YEL
2	F7	2JMF	BLK	RED	BLK	WH
2	F7	2JF1	BLK	GRN	BLK	BLU
2	G1	2JF2	BLK	BRN	BLK	YEL
2	G1	2JDF	BLK	ORG	RED	GRN
2	G2	2KMF	BLK	RED	BLK	WH
2	G2	2LMF	BLK	RED	BLK	WH
2	G3	2LF1	BLK	GRN	BLK	BLU
2	G3	2LF2	BLK	BRN	BLK	YEL
2	G4	2MMF	BLK	RED	BLK	WH
2	G4	2NMF	BLK	RED	BLK	WH

APPENDIX V (cont).

JUNC BOX	TERM BLOCK	GAUGE OR CHAN DESIG	PAIR 1		PAIR 2	
			+EXT	-EXT	+SIG	-SIG
2	G5	2NF1	BLK	GRN	BLK	BLU
2	G5	2NF2	BLK	BRN	BLK	YEL
2	G6	2NDF	BLK	ORG	RED	GRN
2	G6	2NML	RED	WH	RED	BLU
2	G7	2PMF	BLK	RED	BLK	WH
2	G7	2PAL	BLK	GRN	BLK	BLU
2	H1	2QDF1	BLK :	RED	BLK :	WH
2	H1	2QDF2	BLK	GRN	BLK	BLU
2	H2	2QDF3	BLK	BRN	BLK	YEL
2	H2	2QDL	BLK	ORG	RED	GRN
2	H3	2QF1	RED	WH	RED	BLU
2	H3	2QF2	RED	YEL	RED	BRN
1	D2	TSMI	BLK	RED	BLK	WH
1	D2	TSMO	BLK	GRN	BLK	BLU
1	D1	TSRA	BLK	BRN	BLK	YEL
1	D1	TSRB	BLK	ORG	RED	GRN
1	E1	TSRC	RED	WH	RED	BLU
1	E1	TSRT	RED	YEL	RED	BRN

APPENDIX V (cont).

JUNC BOX	TERM BLOCK	GAUGE OR CHAN DESIG	PAIR 1		PAIR 2	
			+EXT	-EXT	+SIG	-SIG
1	E2	TTMI	BLK	RED	BLK	WHT
1	E2	TTMO	BLK	GRN	BLK	BLU
1	E3	TUAI	BLK	RED	BLK	WHT
1	E3	TURA	BLK	GRN	BLK	BLU
1	E4	TURB	BLK	BRN	BLK	YEL
1	E4	TURC	BLK	ORG	RED	GRN
1	E5	TURT	RED	WHT	RED	BLU
1	A1	CHAN1	BLK	RED	WHT	BLK
1	A1	CHAN2	BLK	GRN	BLK	BLU
1	B1	CHAN3	BLK	BRN	BLK	YEL
1	B1	CHAN4	BLK	ORG	RED	GRN
1	C1	CHAN5	RED	WHT	RED	BLU
1	C1	CHAN6	RED	YEL	RED	BRN
1	A2	CHAN7	RED	ORG	GRN	BLU
1	A2	CHAN8	GRN	WHT	GRN	BRN
1	B2	CHAN9	GRN	ORG	GRN	YEL
1	B2	CH 10	WHT	BLU	WHT	BRN

APPENDIX V (cont).

JUNC BOX	TERM BLOCK	GAUGE OR CHAN DESIG	PAIR 1		PAIR 2	
			+EXT	-EXT	+SIG	-SIG
1	C2	CH 11	ORG	WHT	WHT	YEL
1	C2	CH 12	BRN	BLU	BLU	ORG
1	A3	CH 13	BLK	RED	BLK	WHT
1	A3	CH 14	BLK	GRN	BLK	BLU
1	B3	CH 15	BLK	BRN	BLK	YEL
1	B3	CH 16	BLK	ORG	RED	GRN
1	C3	CH 17	RED	WHT	RED	BLU
1	C3	CH 18	RED	YEL	RED	BRN
1	A4	CH 19	RED	ORG	GRN	BLU
1	A4	CH 20	GRN	WHT	GRN	BRN
1	B4	CH 21	GRN	ORG	GRN	YEL
1	B4	CH 22	WHT	BLU	WHT	BRN
1	C4	CH 23	WHT	ORG	WHT	YEL
1	C4	CH 24	BLU	BRN	BLU	ORG
1	D3	CH 25	BLK	RED	BLK	WHT
1	D3	CH 26	BLK	GRN	BLK	BLU
1	D4	CH 27	BLK	BRN	BLK	YEL
1	D4	CH 28	BLK	ORG	RED	GRN

APPENDIX V (cont).

JUNC BOX	TERM BLOCK	GAUGE OR CHAN DESIG	PAIR 1		PAIR 2	
			+EXT	-EXT	+SIG	-SIG
1	D5	CH 29	RED	WHT	RED	BLU
1	D5	CH 30	RED	YEL	RED	BRN
1	D6	CH 31	RED	ORG	GRN	BLU
1	D6	CH 32	GRN	WHT	GRN	BRN
2	A1	CH 33	BLK	RED	WHT	BLK
2	A1	CH 34	BLK	GRN	BLK	BLU
2	B1	CH 35	BLK	BRN	BLK	YEL
2	B1	CH 36	BLK	ORG	RED	GRN
2	C1	CH 37	RED	WHT	RED	BLU
2	C1	CH 38	RED	YEL	RED	BRN
2	A2	CH 39	RED	ORG	GRN	BLU
2	A2	CH 40	GRN	WHT	GRN	BRN
2	B2	CH 41	GRN	ORG	GRN	YEL
2	B2	CH 42	WHT	BLU	WHT	BRN
2	C2	CH 43	ORG	WHT	WHT	YEL
2	C2	CH 44	BRN	BLU	BLU	ORG
2	A3	CH 45	BLK	RED	BLK	WHT
2	A3	CH 46	BLK	GRN	BLK	BLU

APPENDIX V (cont).

JUNC BOX	TERM BLOCK	GAUGE OR CHAN DESIG	PAIR 1		PAIR 2	
			+EXT	-EXT	+SIG	-SIG
2	B3	CH 47	BLK	BRN	BLK	YEL
2	B3	CH 48	BLK	ORG	RED	GRN
2	C3	CH 49	RED	WHT	RED	BLU
2	C3	CH 50	RED	YEL	RED	BRN
2	A4	CH 51	RED	ORG	GRN	BLU
2	A4	CH 52	GRN	WHT	GRN	BRN
2	B4	CH 53	GRN	ORG	GRN	YEL
2	B4	CH 54	WHT	BLU	WHT	BRN
2	C4	CH 55	WHT	ORG	WHT	YEL
2	C4	CH 56	BLU	BRN	BLU	ORG
2	D5	CH 57	BLK	RED	BLK	WHT
2	D5	CH 58	BLK	GRN	BLK	BLU
2	D4	CH 59	BLK	BRN	BLK	YEL
2	D4	CH 60	BLK	ORG	RED	GRN
2	D3	CH 61	RED	WHT	RED	BLU
2	D3	CH 62	RED	YEL	RED	BRN
2	D2	CH 63	RED	ORG	GRN	BLU
2	D2	CH 64	GRN	WHT	GRN	BRN

APPENDIX W.

Color Codes and Pin Connections for Power Cable SJS1

PIN NO	COLOR CODE	SIGNAL
A	WHT	+ 28 VDC Input
B	BLK	+ 28 VDC RTN
C	RED	Case GND

APPENDIX X.

Color Codes and Pin Connections for Signal Cable SJS1

CHAN NO	PAIR NO	COLOR CODE	PIN NO	SIGNAL
1	1	BLK	C	+ Exc
		RED	W	- Exc
	2	WHT	A	+ Data
		BLK	B	- Data
2	3	BLK	r	+ Exc
		GRN	Y	- Exc
	4	BLK	D	+ Data
		BLU	Z	- Data
3	5	BLK	t	+ Exc
		BRN	a	- Exc
	6	BLK	F	+ Data
		YEL	b	- Data
4	7	BLK	J	+ Exc
		ORG	d	- Exc
	8	RED	G	+ Data
		GRN	H	- Data
5	9	RED	M	+ Exc
		WHT	f	- Exc
	10	RED	K	+ Data
		BLU	L	- Data

APPENDIX X (cont).

CHAN NO	PAIR NO	COLOR CODE	PIN NO	SIGNAL
6	11	RED	i	+ Exc
		YEL	x	- Exc
	12	RED	N	+ Data
		BRN	h	- Data
7	13	RED	j	+ Exc
		ORG	z	- Exc
	14	GRN	R	+ Data
		BLU	k	- Data
8	15	GRN	U	+ Exc
		WHT	n	- Exc
	16	GRN	S	+ Data
		BRN	T	- Data
9	17	GRN	q	+ Exc
		ORG	AA	- Exc
	18	GRN	V	+ Data
		YEL	p	- Data
10	19	WHT	u	+ Exc
		BLU	w	- Exc
	20	WHT	e	+ Data
		BRN	v	- Data

APPENDIX X (cont).

CHAN NO	PAIR NO	COLOR CODE	PIN NO	SIGNAL
11	21	ORD	s	+ Exc
		WHT	DD	- Exc
	22	WHT	BB	+ Data
		YEL	CC	- Data
12	23	BRN	y	+ Exc
		BLU	GG	- Exc
	24	BLU	EE	+ Data
		ORG	FF	- Data

APPENDIX Y.

Color Codes and Pin Connections for Signal Cable SJS2

PAIR NO	COLOR CODE	PIN NO	SIGNAL
1	BLK		
	RED	X	Cal Cmd B1
2	BLK	q	Cal Cmd B2
	WHT	AA	Cal Cmd A2
3	BLK	m	Cal Cmd A1
	GRN	p	Cal Cmd Common
4	BLK	u	Frate Out
	BLU	w	Frate Rtn
5	BLK	s	B10 Out
	BRN	DD	B10 Rtn
6	BLK	BB	2 Clk Out
	YEL	CC	2 Clk Rtn
7	BLK	y	NRZL Out
	ORG	GG	NRZL Rtn
8	RED	EE	Oo Clk Out
	GRN	FF	Oo Clk Rtn
9	RED	e	WD Rate Out
	WHT	v	WD Rate Rtn

APPENDIX Y (cont).

CH NO	PAIR NO	COLOR CODE	PIN NO	SIGNAL
13	1	BLK	C	+ Exc
		RED	W	- Exc
	2	BLK	A	+ Data
		WHT	B	- Data
14	3	BLK	r	+ Exc
		GRN	Y	- Exc
	4	BLK	D	+ Data
		BLU	Z	- Data
15	5	BLK	t	+ Exc
		BRN	a	- Exc
	6	BLK	F	+ Data
		YEL	b	- Data
16	7	BLK	J	+ Exc
		ORG	d	- Exc
	8	RED	G	+ Data
		GRN	H	- Data
17	9	RED	M	+ Exc
		WHT	f	- Exc
	10	RED	K	+ Data
		BLU	L	- Data

APPENDIX Y (cont).

CH NO	PAIR NO	COLOR CODE	PIN NO	SIGNAL
18	11	RED	i	+ Exc
		YEL	x	- Exc
	12	RED	N	+ Data
		BRN	h	- Data
19	13	RED	j	+ Exc
		ORG	z	- Exc
	14	GRN	R	+ Data
		BLU	k	- Data
20	15	GRN	U	+ Exc
		WHT	n	- Exc
	16	GRN	S	+ Data
		BRN	T	- Data
21	17	GRN	q	+ Exc
		ORG	AA	- Exc
	18	GRN	V	+ Data
		YEL	p	- Data
22	19	WHT	u	+ Exc
		BLU	w	- Exc
	20	WHT	e	+ Data
		BRN	v	- Data

APPENDIX Y (cont).

CH NO	PAIR NO	COLOR CODE	PIN NO	SIGNAL
23	21	WHT	s	+ Exc
		ORG	DD	- Exc
	22	WHT	BB	+ Data
		YEL	CC	- Data
24	23	BLU	y	+ Exc
		BRN	GG	- Exc
	24	BLU	EE	+ Data
		ORG	FF	- Data

APPENDIX Z.

Color Codes and Pin Connections for Signal Cable SJS3

CH NO	PAIR NO	COLOR CODE	PIN NO	SIGNAL
25	1	BLK	C	+ Exc
		RED	W	- Exc
	2	BLK	A	+ Data
		WHT	B	- Data
26	3	BLK	r	+ Exc
		GRN	Y	- Exc
	4	BLK	D	+ Data
		BLU	Z	- Data
27	5	BLK	t	+ Exc
		BRN	a	- Exc
	6	BLK	F	+ Data
		YEL	b	- Data
28	7	BLK	J	+ Exc
		ORG	d	- Exc
	8	RED	G	+ Data
		GRN	H	- Data
29	9	RED	M	+ Exc
		WHT	f	- Exc
	10	RED	K	+ Data
		BLU	L	- Data

APPENDIX Z (cont).

CH NO	PAIR NO	COLOR CODE	PIN NO	SIGNAL
30	11	RED	i	+ Exc
		YEL	x	- Exc
	12	RED	N	+ Data
		BRN	h	- Data
31	13	RED	j	+ Exc
		ORG	z	- Exc
	14	GRN	R	+ Data
		BLU	k	- Data
32	15	GRN	U	+ Exc
		WHT	n	- Exc
	16	GRN	S	+ Data
		BRN	T	- Data

DISTRIBUTION:

Amarillo College
Amarillo, TX 79100
Attn: E. Gilmore

Battelle-Pacific Northwest
Laboratory
P.O. Box 999
Richland, WA 99352
Attn: L. Wendell

Monique Carpentier
Energy, Mines and Resources
Renewable Energy Branch
460 O'Connor St.
Ottawa, Ontario
CANADA K1A OE4

DOE/ALO/ETWMD
Albuquerque, NM 87115
Attn: G. P. Tennyson

DOE Headquarters (5)
Wind/Oceans Technologies Division
1000 Independence Avenue
Washington, DC 20585
Attn: L. J. Rogers
P. R. Goldman

Fayette Manufacturing Corporation
P.O. Box 1149
Tracy, CA 95378-1149
Attn: W. Thompson

FloWind Corporation (2)
1183 Quarry Lane
Pleasanton, CA 94566
Attn: L. Schienbein
B. Im

A. D. Garrad
Garrad Hasson
10 Northampton Square
London EC1M 5PA
UNITED KINGDOM

Dr. I. J. Graham
Southern University
Department of Mechanical
Engineering
P.O. Box 9445
Baton Rouge, LA 70813-9445

HiTec Corp.
Nadrone Industrial Park
65 Powers Road
Westfond, MA 01886
Attn: R. A. Sabean

Indal Technologies, Inc. (2)
3570 Hawkestone Road
Mississauga, Ontario
CANADA L5C 2V8
Attn: D. Malcolm
C. Wood

Institut de Recherche d'Hydro-Quebec
1800, Montee Ste-Julie
Varennes, Quebec, JOL 2P.O.
CANADA
Attn: Bernard Masse

K. Jackson
West Wind Industries
P.O. Box 1705
Davis, CA 95617

R. E. Kelland
The College of Trades and Technology
P.O. Box 1693
Prince Philip Drive
St. John's, Newfoundland, AlC 5P7
CANADA

Kinetics Group, Inc.
P.O. Box 1071
Mercer Island, WA 98040
Attn: J. Sladky, Jr.

G. M. McNerney
US Wind Power
160 Wheeler Road
Burlington, MA 01803

New Mexico Engineering
Research Institute (2)
Campus P.O. Box 25
Albuquerque, NM 87131
Attn: G. G. Leigh
D. Morrison

Ohio State University
Aeronautical and Astronautical Dept.
2070 Neil Avenue
Columbus, OH 43210
Attn: Professor G. Gregorek

Oklahoma State University
Mechanical Engineering Dept.
Stillwater, OK 76074
Attn: D. K. McLaughlin

Pacific Gas & Electric Co.
3400 Crow Canyon Road
San Ramon, CA 94583
Attn: T. Hillesland

Ion Paraschivoiu
Department of Mechanical
Engineering
Ecole Polytecnique
CP 6079
Succursale A
Montreal H3C 3A7
CANADA

Jacques Plante
Shawinigan Consultants, Inc.
620 Dorchester Blvd. West
Montreal, Quebec
CANADA H3B 1N8

RANN, Inc.
260 Sheridan Ave., Suite 414
Palo Alto, CA 94306
Attn: A. J. Eggers, Jr.

Dr. R. Ganesh Rajagopalan,
Asst. Prof.
Aerospace Engineering Department
Iowa State University
404 Town Engineering Bldg.
Ames, IA 50011

R. G. Richards
Atlantic Wind Test Site
P.O. Box 189
Tignish P.E.I., COB 2BO
CANADA

Gwen Schreiner
Librarian
National Atomic Museum
Albuquerque, NM 87185

Solar Energy Research Institute
1617 Cole Boulevard
Golden, CO 80401
Attn: R. W. Thresher

Peter South
ADECON
32 Rivalda Road
Weston, Ontario, M9M 2M3
CANADA

Stanford University
Dept. of Aeronautics and Astro
Mechanical Engineering
Stanford, CA 94305
Attn: Holt Ashley

Dr. Derek Taylor
Alternative Energy Group
Walton Hall
Open University
Milton Keynes, MK7 6AA
UNITED KINGDOM

R. Rangi (2)
Low Speed Aerodynamics Laboratory
NRC-National Aeronautical
Establishment
Montreal Road
Ottawa, Ontario, K1A 0R6
CANADA

Texas Tech University
Mechanical Engineering Dept.
P.O. Box 4289
Lubbock, TX 79409
Attn: J. W. Oler

University of Massachusetts
Mechanical and Aerospace
Engineering Dept.
Amherst, MA 01003
Attn: Dr. D. E. Cromack

University of Oklahoma
Aero Engineering Department
Norman, OK 73069
Attn: K. Bergey

USDA, Agricultural Research Service
Southwest Great Plains Research
Center
Bushland, TX 79012
Attn: Dr. R. N. Clark
R. Davis

W. A. Vachon
W. A. Vachon & Associates
P.O. Box 149
Manchester, MA 01944

Washington and Lee University
P.O. Box 735
Lexington, VA 24450
Attn: Dr. R. E. Akins

West Texas State University
Government Depository Library
Number 613
Canyon, TX 79015

West Texas State University
Department of Physics
P.O. Box 248
Canyon, TX 79016
Attn: V. Nelson

West Texas State University
Dept. of Aero Engineering
1062 Kountz Avenue
Morgantown, WV 26505
Attn: R. Walters

West Virginia University
Dept. of Aero Engineering
1062 Kountz Avenue
Morgantown, WV 26505
Attn: R. Walters

400	R. C. Maydew
1520	L. W. Davison
1522	R. C. Reuter, Jr.
1522	D. W. Lobitz
1522	E. D. Reedy
1523	J. H. Biffle
1524	A. K. Miller
1524	C. R. Dohrmann
1524	P. S. Veers
1550	C. W. Peterson
1552	J. H. Strickland
1556	G. F. Homicz
3141	S. A. Landenberger (5)
3151	W. I. Klein (3)
3154-3	C. H. Dalin (8) For DOE/OSTI (Unlimited Release)
3160	J. E. Mitchell (15)
3161	P. S. Wilson
6000	D. L. Hartley
6200	V. L. Dugan
6220	D. G. Schueler
6225	H. M. Dodd (50)
6225	T. D. Ashwill
6225	D. E. Berg
6225	T. C. Bryant
6225	P. C. Klimas
6225	S. D. Nicolaysen
6225	M. E. Ralph
6225	D. C. Reda
6225	M. A. Rumsey
6225	L. L. Schluter
6225	W. A. Stephenson (5)
6225	H. J. Sutherland (10)
7544	D. O. Smallwood
7544	T. G. Carne
7544	J. Lauffer
8524	P. W. Dean